NSG 5348

EVIDENCE FOR MAGNETIC FIELD RECONNECTION AT THE EARTH'S MAGNETOPAUSE

B.U.Ö. Sonnerup[1], G. Paschmann[2], I. Papamastorakis[2], N. Sckopke[2], G. Haerendel[2], S.J. Bame[3], J.R. Asbridge[3], J.T. Gosling[3], and C.T. Russell[4]

20 January 1981

(1) Dartmouth College, Hanover, N.H. 03755, USA
(2) Max-Planck-Institut für Physik und Astrophysik, Institut für extraterrestrische Physik, 8046 Garching, W-Germany
(3) Los Alamos Scientific Laboratory, Los Alamos, N.M. 87545, USA
(4) University of California at Los Angeles, Institute of Geophysics and Planetary Physics, Los Angeles, CA 90024, USA

ABSTRACT

Eleven passes of the ISEE satellites through the frontside terrestrial magnetopause (local time 9 - 17 h; GSM latitude 2^{o} - 43^{o} N) have been identified, where the plasma velocity in the magnetopause and boundary layer was substantially larger than in the magnetosheath. This paper examines the nature of the plasma flow, magnetic field, and energetic-particle fluxes in these regions, with a view to determining whether the velocity enhancements can be explained by magnetic-field reconnection. The principal question is whether the observed difference in tangential plasma velocity, $\Delta\underline{v}$, between a point in the magnetopause or boundary layer and a reference point in the adjacent magnetosheath, had the direction and magnitude, $\Delta\underline{v}_{theory}$, produced by the Maxwell stresses in the magnetopause, assuming that the magnetosheath plasma moved across that boundary. Except for its sign, $\Delta\underline{v}_{theory}$ is shown to be independent of the normal magnetic field component B_n and flow component v_n . For the 11 cases, the average ratio $|\Delta\underline{v}|/|\Delta\underline{v}|_{theory}$ was in the range 0.6 - 1.2, with a composite average of 0.8. The average angular error was $< 25^{o}$, with a composite average of 10^{o}. The plasma results would require 10 of the crossings to have been located north of the reconnection line $(B_n < 0)$, and one (at 2.4^{o} N lat.) south of it $(B_n > 0)$. The B_n values obtained from minimum-variance analysis of the magnetic data were mostly poorly determined, but in general their signs were consistent with the plasma results. The flow velocity across the magnetopause was also poorly determined but it had a negative (inward) composite average as expected. In several cases energetic magnetospheric particles with the proper flow anisotropy, and, in one case, reflected magnetosheath particles,

were observed outside but adjacent to the magnetopause. All of these results support the reconnection hypothesis. The energetic particles were also used to identify the outer separatrix surface. In one case, it was possible to conclude from its location relative to the magnetopause that the reconnection site was in the vicinity of the equatorial plane and not in the cusp. The electric field tangential to the magnetopause is inferred to be in the range 0.4 - 2.8 mV/m.

1. INTRODUCTION

Ever since its introduction into magnetospheric physics by Dungey (1961), the concept of magnetic field reconnection has played a central role in most attempts to provide a unified theoretical framework upon which to place a multitude of observations relevant to the large-scale dynamics of the magnetosphere (e.g., Axford, 1969). Yet the process itself has remained something of an enigma, and the subject of considerable controversy (Heikkila, 1975; Alfvén, 1976), fueled, in part by claims of a lack of direct and incontrovertible observational evidence for its occurrence, in part by objections to the mode of description ("moving field lines") and analysis (MHD) of the process, leading some to conclude that the process is an encumbrance rather than an aid in understanding magnetospheric physics, and in part by questions concerning the real nature of reconnection and the parameters that influence its occurrence and efficiency.

The first source of controversy is the principal subject of this paper. Specifically, we shall use plasma, magnetic field, and energetic particle data from the ISEE mission to present direct and powerful, if not incontrovertible, evidence for the occurrence of reconnection at the magnetopause. The primary evidence consists of observations of high speed plasma in the magnetopause and boundary layer and of a demonstration that the observed plasma velocities are in approximate quantitative agreement with the predictions of the reconnection model. A brief report on one event has been given earlier (Paschmann et al., 1979, hereafter referred to as paper 1). In the present paper we examine ten more cases, using the same basic approach as in paper 1, but with the added use of higher energy particles and reflected particles to provide independent evidence concerning the field line topology near the magnetopause.

For the most part, we shall not get embroiled in the second controversy, that concerning the terminology and approach used in discussing and analyzing reconnection. However, two observations on this matter are in order. First, reconnection can be defined in a manner that does not involve "frozen-fields" or MHD terminology: reconnection occurs when an electric field is present along a magnetic separator (X-line, reconnection line) in a plasma. Thus, the fact that most theories of reconnection have used the MHD approach and associated language, does not necessarily mean that the process exists only in the minds of those using the MHD approach. It can be discussed, albeit at some inconvenience, without the use of phrases such as "moving field lines" or "magnetic flux transfer". The name "reconnection" itself does, of course, have its roots in the frozen-field concept, but those who find it offensive may use the more innocuous term "merging" without creating communication difficulties. Second, we shall demonstrate that certain predictions of simple MHD reconnection models, specifically the occurrence of plasma acceleration at the magnetopause, are borne out by the observations to be presented here. While these results by no means prove that MHD offers an adequate description of all aspects of magnetopause reconnection (it almost certainly does not), they, at least, demonstrate that MHD models can serve as a useful guide in the interpretation of certain basic magnetopause observations. The reason is that MHD, after all, is based on simple conservation laws, which have global validity even when MHD fails to provide an accurate description in certain narrow local regions, such as the interior of the magnetopause.

The third category of controversy is concerned, not with the occurrence or validity of the reconnection process, but with its actual physical characteristics. Our study has a strong bearing on some of the questions

raised in this area. Does reconnection as it actually occurs at the magnetopause ever bear any similarity to the simple two-dimensional time-independent models used to describe it or is it dominated by three-dimensional and/or time-dependent effects? Does magnetopause reconnection occur whenever the magnetosheath magnetic field turns south or are there other conditions and thresholds for its appearance? How large are the reconnection rates? Is the reconnection site located near the equatorial plane as originally visualized by Dungey or in one (or both) of the cusps (Haerendel et al., 1978) or perhaps elsewhere (Crooker, 1979)? Do energy transport mechanisms such as electron and ion heat conduction or MHD waves play an important role?

The paper is organized as follows. Section 2 contains a review of the simple reconnection model with which the data will be compared. Section 3 lists and discusses a number of theoretical predictions and tests. The instrumentation and data reduction are discussed in Section 4. Section 5 contains the main presentation of the observations. In this section, time records of sample crossings are shown and discussed; the tests developed in Section 3 are applied (data selection criteria for these tests are given in the Appendix); and a discussion of our predictions concerning the magnitude of the reconnection electric field is given. Finally, Section 6 contains a summary and discussion of the results.

2. THE RECONNECTION PROCESS

For detailed reviews of the reconnection process the reader is referred to the papers by Vasyliunas (1975) and Sonnerup (1979). In this section, we summarize those aspects of reconnection that are important for our data interpretation. The MHD reconnection model with which we shall compare the

ISEE observations was proposed by Levy et al. (1964) (see also Petschek (1966) and Yang and Sonnerup (1977)). It is a steady-state two-dimensional geometry in which the magnetopause appears as a rotational discontinuity ("intermediate wave") having a finite normal magnetic field component B_n so that the magnetosheath and magnetosphere field lines are connected across the magnetopause in the manner shown in Figure 1a. The reconnection site in that figure is the line (separator, or X-line) in the equatorial plane (i.e. perpendicular to the plane of the figure) where two magnetic field surfaces, referred to as the separatrices, intersect each other, implying a null in the field. These surfaces have topological significance in that they separate regions in which the magnetic field lines have two feet, one foot, and no feet, on the earth.

In Figure 1a, magnetosheath plasma is imagined to move to the right toward the magnetosphere. Most of it flows around the obstacle but a fraction crosses the magnetopause as a result of the presence of the normal field B_n . This component is negative, i.e. directed towards the earth, north of the separator, and positive south of it. The theory of the rotational discontinuity indicates the normal flow speed to be the Alfvén speed based on B_n . The flow is not field-aligned but takes place along streamlines, shown as dashed lines in Figure 1a, which cross the magnetic field. Such cross-field flow requires the presence of an electric field $\underline{E}_t$, tangential to the magnetopause, and along the separator. Thus, according to the definition given in the introduction, reconnection occurs at that line. It may be shown that $\underline{E}_t$ is proportional to the magnitude of the normal magnetic field component B_n.

The reconnection electric field $\underline{E}_t$ is also seen to be aligned with the Chapman-Ferraro magnetopause current $\underline{I}$ so that $\underline{E}_t \cdot \underline{I} > 0$. Such a

situation implies the conversion of electromagnetic energy into other forms, presumably plasma energy. In the present MHD model this energy is carried away in high-speed plasma jets flowing away from the reconnection site in two wedge-shaped regions attached to the inside of the magnetopause and with vertices at the separator. It is important to note that only a minute fraction of these jets, namely the layer closest to the earth, contains magnetosheath plasma that has passed through the region immediately adjacent to the reconnection site, the so-called diffusion region. Most parts of the jets are populated by plasma that has crossed the magnetopause away from the diffusion region, and in doing so, has been accelerated by the $\underline{I} \times \underline{B}_n$ force. It is evident from Figure 1 that the acceleration is tangential to the magnetopause and directed away from the reconnection site. These jets are the principal feature of the reconnection process with which this paper is concerned. And it was the absence of observations of such high-speed plasmas that led Heikkila (1975) to conclude that reconnection does not occur at the magnetopause, while Haerendel et al. (1978) circumvented this conclusion by suggesting the polar cusps as the reconnection site. Heikkila described the situation as an energy crisis. But more fundamentally it is a tangential momentum crisis,for without changing the plasma momentum at the magnetopause there can be no $\underline{I} \times \underline{B}_n$ force, i.e., B_n must be zero. And without finite B_n there is no reconnection.

The flow speed in the plasma jets is independent of the magnitude, E_t, of the reconnection electric field. If E_t is small, the jets are narrow and entail a small total particle flux. The plasma ions in the jets have picked up their energy by drifting a substantial distance along $\underline{E}_t$ as they crossed the magnetopause. This large drift displacement occurs be-

cause B_n is small. As E_t, and with it B_n, increases, the wedge angle and particle flux increase, and the ion drift displacement along E_t decreases, but the ions gain exactly the same amount of energy as before.

For conditions expected at the magnetopause, the jets are very narrow: up to a distance (along the magnetopause) of 2-3 R_E from the separator, their width should remain comparable to the magnetopause thickness (e.g., Yang and Sonnerup, 1977). For this reason plasma data with high time resolution are needed.

A schematic of the type shown in Figure 1a is incomplete in that it assumes the magnetosheath field to be exactly antiparallel to the earth's field in the equatorial plane, which is usually not the case. However, it is believed the reconnection may proceed even if the magnetosheath magnetic field has a B_y component. This is a principal reason why the magnetopause in this model consists of a rotational discontinuity, that being the only one of the MHD discontinuities with $B_n \neq 0$ capable of rotating the tangential component of the magnetic field vector by an arbitrary angle (even when $B_y = 0$ in the magnetosheath, $B_y \neq 0$ is expected to occur as part of the magnetopause structure). It is thought that a positive B_y tilts the separator so that it is located south of the equatorial plane on the prenoon side, north of that plane on the postnoon side of the magnetopause; a negative B_y yields the opposite tilt (see, for example, Gonzalez and Mozer, 1975). Furthermore, a tilted separator ceases to be a magnetic null line but, along with the separatrices, it retains its other topological properties. Figure 1b illustrates the situation, as seen from the sun, for $B_y > 0$. The separator may also be limited in longitude, perhaps to a relatively narrow segment, a feature not shown in the figure.

Except in unusual circumstances, a satellite crossing the magnetopause will not encounter the site of reconnection itself, the diffusion region. Rather it will penetrate the current layer away from that region and thus, according to the model just described, it will pass through a rotational discontinuity. On the other hand, if no reconnection takes place, the magnetopause should be a tangential discontinuity which by definition has $B_n = 0$. Furthermore, E_t should then also vanish very nearly and at most a diffusive leakage of magnetosheath plasma should occur across the magnetopause. In order to discriminate between the two types of discontinuity it is in principle sufficient to establish the presence or absence of B_n. Efforts to do so by use of magnetic field measurements alone have been reported (e.g. Sonnerup and Ledley, 1979) and, in isolated instances, the presence of significant B_n values has been established beyond reasonable doubt. However, for most crossings the magnetic results alone are not convincing and for this reason it is necessary to examine plasma data along with the magnetic data. The theoretical predictions upon which to base such an examination are summarized in the next section. They are extracted from the work of Hudson (1970, 1971, 1973) concerning the jump conditions across rotational and other discontinuities in a gyrotropic plasma.

3. THEORETICAL PREDICTIONS AND TESTS

The basic assumption underlying existing theoretical models of the rotational discontinuity is that it can be treated as a one-dimensional time-independent structure. When such models are compared with the actual magnetopause it must be remembered that the structure of the latter often has substantial two and three-dimensional features and that the situation

seldom, if ever, is time-independent. For this reason one should not expect that the theoretical tests, given below, will ever be exactly met by any magnetopause data set. Rather, one must judge whether the observations agree with the theory to a sufficient degree so that one has confidence that the latter does in fact contain the dominant physical process operative in the magnetopause. For the rotational discontinuity, that process is the tangential acceleration of plasma by the $\underline{I} \times \underline{B}_n$ force.

A second point is that to date the rotational discontinuity has been analyzed only in terms of the jump conditions across it. No general theory exists that predicts its structure and thickness in a collision-free plasma (a special case has been treated by Su and Sonnerup, 1968). For this reason we shall attempt to use the jump conditions between a reference point in the magnetosheath, denoted by the subscript 1, and those points within the magnetopause structure, as well as on the magnetospheric side of it, at which valid plasma measurements are available. These points will be denoted by the subscript 2. We recognize that for sufficiently thin structures certain additional terms which do not appear in the jump conditions should be included in order for the equations to be applicable to points in the magnetopause (and, because the boundary layer is very thin, probably there also). In particular, shear stresses derived from finite gyroradius effects, and Hall-current terms will appear. These effects are small when $\lambda_i/h \ll 1$ or $R_{Li}/h \ll 1$ where λ_i is the ion inertial length, R_{Li} the ion gyroradius, and h the magnetopause (or boundary layer) thickness. Because the magnetopause motion relative to the satellite is usually not well known, we cannot determine h in a reliable manner for all of the events to be dealt with here. Thus we cannot establish how well the above inequalities are satisfied in each case.

However, on the basis of an average magnetopause thickness in the range 400-800 km reported by Elphic and Russell (1979), it is reasonable to assume that the correction terms, while present and perhaps even substantial, are still sufficiently small to justify their neglect for the purposes of the present paper. Again, the implication is that an approximate rather than exact agreement between "theory" and observations should be expected.

As shown by Hudson (1970), the constancy of the tangential electric field across any discontinuity, combined with the conservation of mass flux, $G = (v_n - U_n)$, leads to the formula

$$B_n (\underline{v}_{2t} - \underline{v}_{1t}) = G (\underline{B}_{2t}/\rho_2 - \underline{B}_{1t}/\rho_1) \qquad (1)$$

provided the tangential electric fields at locations 1 and 2 are expressible as

$$\underline{E}_t = - [(\underline{v} - U_n \underline{n}) \times \underline{B}]_t \qquad (2)$$

Here ρ , $\underline{v}$, and $\underline{B}$ are the mass density, plasma velocity in the satellite frame, and magnetic field, respectively. Subscripts n and t refer to components normal and tangential to the magnetopause; the normal vector $\underline{n}$ is directed outward from the earth. The magnetopause normal velocity relative to the satellite is $U_n = U_{n1} = U_{n2}$.

The conservation of tangential momentum in a nonisotropic plasma may be expressed as

$$G (\underline{v}_{2t} - \underline{v}_{1t}) = (B_n/\mu_o) [\underline{B}_{2t} (1-\alpha_2) - \underline{B}_{1t} (1-\alpha_1)] \qquad (3)$$

where the pressure anisotropy factor α is defined by

$$\alpha = (p_{\parallel} - p_{\perp}) \mu_o / B^2 \quad , \qquad (4)$$

$p_\parallel$ and $p_\perp$ being total plasma pressures parallel and perpendicular to the magnetic field; μ_o denotes the free space permeability. For a rotational discontinuity, the vectors $\underline{B}_{2t}$ and $\underline{B}_{1t}$ are not colinear. In that case, elimination of $(\underline{v}_{2t} - \underline{v}_{1t})$ between (1) and (3) yields

$$(v_n - U_n) = \pm B_n [(1 - \alpha) / \mu_o \rho]^{1/2} \qquad (5)$$

i.e., the normal flow speed into (subscript 1) and out of (subscript 2) the discontinuity is equal to the Alfvén speed based on the normal field component, and corrected for the pressure anisotropy. Using Eq. (5), the conservation of mass, $G_1 = G_2 = G$, then yields

$$\rho_1 (1 - \alpha_1) = \rho_2 (1 - \alpha_2) \qquad (6)$$

and Eqs. (1) and (3) take on the identical form

$$(\underline{v}_{2t}-\underline{v}_{1t}) = \pm [\rho_1(1-\alpha_1)/\mu_o]^{1/2}(\underline{B}_{2t}/\rho_2-\underline{B}_{1t}/\rho_1) \qquad (7)$$

Assuming $G < 0$, the positive and negative signs in (5) and (7) correspond to $B_n < 0$ and $B_n > 0$, respectively.

Equation (7) indicates that the tangential plasma velocity difference is equal to the tangential Alfvén velocity difference.

I. Tangential Component Test. Equation (1) forms the basis of the following tests:

(Ia) If B_n and G are nonzero, as in a rotational discontinuity, then all the measured difference vectors $\Delta\underline{v}_t = (\underline{v}_{2t} - \underline{v}_{1t})$ and $\Delta\underline{B}_t/\rho = (\underline{B}_{2t}/\rho_2 - \underline{B}_{1t}/\rho_1)$ for a magnetopause crossing should be colinear.

(Ib) Assuming plasma flow from the magnetosheath into the magnetosphere

($G < 0$), the vectors $\Delta\underline{v}_t$ and $\Delta\underline{B}_t/\rho$ should be consistently parallel for crossings north of the separator where $B_n < 0$, and antiparallel south of that line where $B_n > 0$.

By use of Eq. (7) the magnitude relationship between $|\Delta\underline{v}_t|$ and $|\Delta\underline{B}_t/\rho|$ can also be tested observationally:

(Ic) Across a rotational discontinuity the tangential velocity difference vectors should have the magnitude $[\rho_1 (1 - \alpha_1) / \mu_o]^{1/2} |\Delta\underline{B}_t/\rho|$.

Several comments should be made about the tangential component tests because they form the principal basis for the identification of reconnection events in this paper. First, test (Ia) indicates that approximate colinearity of the vectors $\Delta\underline{v}_t$ and $\Delta\underline{B}_t/\rho$ is a strong indication of the presence of nonvanishing values of B_n and G. For a tangential discontinuity no such relationship is expected. Unless B_n and G both happened to change sign together, test (Ib) indicates that persistent parallelarity or antiparallelarity of all the pairs of difference vectors $(\Delta\underline{v}_t , \Delta\underline{B}_t/\rho)$ in a crossing means that B_n had a persistent sign during the crossing - negative in the former case, positive in the latter. By contrast, the convection of one or more X-lines past the satellite would lead to alternating parallel and antiparallel difference vector pairs. Finally, test (Ic) allows one to check whether the tangential velocity change across the magnetopause has the correct magnitude to have been caused by the $\underline{I} \times \underline{B}_n$ force.

A second comment is that Eq. (7) does not contain B_n, v_n, or U_n, all of which are difficult to determine accurately from the measurements.

Furthermore, the tangential components of $\underline{v}$ and $\underline{B}$ are relatively insensitive to the choice of the magnetopause normal vector. In fact, Hudson (1970) has pointed out that Eq's. (1) and (7) are also valid for the total difference vectors $\Delta\underline{v}$ and $\Delta(\underline{B}/\rho)$, so that no reference to the normal direction is needed.

Finally, note that the tests are local in nature. In other words, it is assumed that in crossing the magnetopause the magnetosheath plasma seen at some location inside that layer experienced the magnetopause magnetic field structure at that latitude and longitude. Clearly, such would not be the case for the plasma at the inner edge of the plasma jets in Figure 1a which presumably crossed the magnetopause in or near the diffusion region, i.e. far away from the satellite location. Furthermore, for extremely small values of B_n (0.1 nT, say) the drift displacement of ions crossing the magnetopause would be sufficiently great to violate the local hypothesis.

II. Normal Component Tests. Under favorable circumstances, the magnetopause normal vector, $\underline{n}$, and normal field component, B_n, can be determined directly from the magnetic field data by use of minimum variance analysis. In that case the following tests may be made:

(IIa) Does the sign of B_n agree with that predicted by test Ib?

(IIb) Does $(v_n - U_n)$, calculated by using the minimum variance normal and the best estimate of U_n, indicate the expected inward plasma flow across the magnetopause?

(IIc) In case reasonably reliable average values are obtained for B_n and $(v_n - U_n)$ for a crossing, is the value of the latter in satisfactory agreement with that predicted by Eq. (5)?

Experience indicates that B_n values obtained from the minimum variance method and v_n values derived by projection of measured plasma flow vectors along $\underline{n}$ often have large uncertainties. Thus, test II can rarely be performed on an individual crossing. In the observation section we shall use this set of tests with values of B_n and v_n formed by averaging over several crossings.

III. Topology Tests. If the magnetic field at the magnetopause does in fact have the topology shown in Figure 1a then one might expect the regions in space, outside the magnetopause but inside the outer separatrix surface, to have signatures indicating that the magnetic field lines cross the magnetopause and are connected with the earth. On that basis the following two tests arise:

(IIIa) Is there evidence of energetic (or other) ions of magnetospheric origin in a layer outside the magnetopause, and if so, do these particle fluxes have the expected anisotropy? In other words, do they stream in the direction antiparallel to $\underline{B}$ when $B_n < 0$ (i.e., north of the separator), parallel to $\underline{B}$ when $B_n > 0$ (south of the separator)?

(IIIb) Is there evidence of reflection of some magnetosheath particles at the magnetopause, and if so, do these particles have the expected tangential velocity change, given by

$$\Delta \underline{v}_t = \pm 2\, \underline{B}_{t1} \left[(1 - \alpha_1) / \mu_o \rho_1 \right]^{1/2} \qquad (8)$$

(This formula is obtained by putting $\underline{B}_{t2} = - \underline{B}_{t1}$ in Eq. (7); the upper and lower signs refer to $B_n < 0$ and $B_n > 0$, respectively.)

Neither of the effects dealt with in these two tests is a necessary signature of reconnection. One may imagine the process to occur without any associated substantial leakage of magnetospheric particles (except perhaps right at the separatrix) and without any substantial reflection of magnetosheath particles. But when one or both effects are present, they add confidence to the identification of reconnection events based on tests I and II.

Test III has been applied by Scholer et al. (1981) to a few ISEE-1 crossings. It may be noted that the region between the inner separatrix and the magnetopause may occasionally also have energetic particle signatures indicative of reconnection (e.g., Williams and Frank, 1980). This latter aspect is not explored in the present paper.

Other Tests. In principle, the jump conditions across a rotational discontinuity permit of several additional consistency tests. For example, Hudson (1971, 1973) has shown that certain restrictions exist on permissible anisotropies α_1 and α_2, and on β_1, the ratio of average plasma pressure to magnetic pressure. Also, when heat flux effects are negligible, the field magnitude ratio B_2/B_1 across a rotational discontinuity can be calculated from those three parameters. However, in the cases to be considered here the physical situation was not sufficiently clean and the measurements not sufficiently accurate to permit of a meaningful comparison between those theoretical predictions and the observations.

Tangential Electric Field. A final item to be dealt with in this summary of theoretical results is the electric field, $\underline{E}_t$, tangential to the magnetopause. In any two-dimensional model of reconnection, the component of this field along the separator is a direct measure of the reconnection rate. We shall calculate $\underline{E}_t$ from Eq. (2), recognizing that the Hall current term, which is not included, may make a substantial contribution at points within the magnetopause (and at the inner edge of the boundary layer as well). Upon use of Eq. (5) for the normal flow $(v_n - U_n)$ we find

$$\underline{E}_t = B_n \underline{n} \times \{\underline{v}_t \mp (\underline{B}_t/\rho)[(1 - \alpha_1)\, \rho_1/\mu_o]^{1/2}\} . \qquad (9)$$

where the upper and lower signs refer to $B_n < 0$ and $B_n > 0$, respectively. This formula establishes the result quoted earlier that the electric field is directly proportional to B_n. Since the latter quantity is usually difficult to determine accurately, it is correspondingly difficult to obtain an accurate estimate of the electric field magnitude. On the other hand, the direction of $\underline{E}_t$ can be determined via Eq. (9). Using an average B_n for several crossings, the magnitude of E_t can then be estimated.

The component of $\underline{E}_t$ along the separator can be established only if the orientation of the latter is known. If one assumes that line to be parallel to the magnetopause current $\underline{I}$ (as has been done by Gonzalez and Mozer, 1975, and many others) then the "reconnection component" of $\underline{E}_t$ may be readily ascertained. But reconnection geometries have also been proposed in which such alignment is not at hand (Cowley, 1976; contrary to a statement in paper 1, a finite angle between $\underline{E}_t$ and $\underline{I}$ does not necessarily provide support for such geometries).

The component of $\underline{E}_t$ perpendicular to the separator is associated with plasma flow and magnetic field components along it.

4. INSTRUMENTATION AND DATA REDUCTION

The observations discussed in this paper were obtained with the LASL/MPI fast plasma experiments and the UCLA magnetometer experiments on the ISEE-1 and -2 satellites, which are in elliptical orbits around the earth, with apogees near 22.5 R_E (Ogilvie et al., 1977).

The fast plasma experiment (Bame et al., 1978) consists of three 90^o spherical section electrostatic analyzers. Measurements of ions and electrons are taken in 16 contiguous energy per charge intervals as the analyzer plate voltage decays exponentially in ~188 ms. For ions, which we are exclusively concerned with in this paper, the energy range employed in the magnetopause region extends from 70 eV up to 40 keV.

Two of the analyzers make two-dimensional (2D) measurements in which the instruments integrate between -55^o and $+55^o$ in elevation angle relative to the satellite equatorial plane or, nearly equivalently, ecliptic latitude, while sampling approximately every 22.5^o in azimuth angle (longitude). A complete 2D distribution of ions and electrons is accumulated in one spin (~ 3 s), and is repeated every 3s or 12s at high and low bit rate, respectively.

The third analyzer makes three-dimensional (3D) measurements by sequentially sampling each of four elevation angle segments (of 27.5^o width) extending over the same range (-55^o to $+55^o$) as the 2D analyzers. With this range of elevation angles, 82% of the solid angle sphere is viewed by the instruments. The inner two elevation channels are sampled every 45^o in azimuth, the outer two every 90^o. A full 3D distribution is

accumulated in 9s. During the next measurement, another azimuth angle set, interleaved with the first, is obtained. As the instrument operation is synchronized with the telemetry clock, the complete azimuth sampling pattern slowly rotates with time. Full 3D distributions are repeated every 12s or 48s at high and low bit rate, respectively.

Due to the way switching of the four elevation segments is achieved, there is an inherent background effect in the sense that a fraction of the particles incident on the three "off" segments will contribute to the count rate of the one segment being sampled (Bame et al., 1978; Paschmann et al., 1978). As determined from extensive laboratory and regularly spaced in-flight calibration, that fraction varies between 0.12 at 80 eV to a constant 0.18 to 3 keV and above (for ions). Knowledge of the count rates of each elevation angle segment at any given energy and azimuth angle then allows the background to be subtracted. Since the azimuth angle pattern rotates while the elevation channels are being sampled sequentially, some interpolation between count rates is involved. The generally good agreement of the densities computed from the 3D data with the densities from the 2D data (which do not suffer from this background effect) is proof that the method works satisfactorily.

The plasma data are primarily presented as moments of the distribution functions. To calculate these moments, a number of assumptions are made, which mainly concern the derivation of the phase space densities f from the measured count rates and the behaviour of f for elevation angles outside the range of the instruments (for details, see Paschmann et al., 1978).

We used the 2D densities in all quantitative applications because the lack of a background effect makes them more accurate. Simulations with

convected Maxwellian distributions have shown that, for temperatures above 3×10^6 K (the lowest temperatures measured inside the high-velocity regions) and bulk speeds up to ~ 300 km s^{-1}, the 2D densities have relative errors of less than 20% for true flow elevations up to 60^o. (Degradations in multiplier gain, although approximately corrected for, can lead to absolute uncertainties in the densities of up to 40%.)

For the same temperatures and bulk speeds, the 3D flow velocity is correct to within ~20%, as along as the elevation angle of the flow is less than ~60^o. The errors are such as to systematically lower the measured velocity, in particular its component along the spin axis. At larger elevation angles the errors become rapidly larger. Therefore, we have excluded from any quantitative analysis all measurements with apparent flow elevations greater than 55^o (see Appendix).

The pressure tensor (and thus the pressure anisotropy) is not well deteremined by the 3D instrument as soon as the magnetic field direction approaches alignment with the satellite spin axis, which invariably occurs inside the magnetopause. This is again due to the limited angular coverage. However, for the small elevation angles of the magnetic field, which, except for one case, prevailed outside the magnetopause, the pressure anisotropy can be obtained directly, and fairly accurately, from the 2D data. As shown in Section 3, the anisotropy in the magnetosheath is all that is needed in the analysis.

In determining velocities from the measured energy/charge, we have assumed the ions to be protons. Any admixture of alpha-particles will modify the moments, but as long as the alpha abundance is 10% or less, the effect on the velocity will be small. However, with their four times higher mass, the alpha-particles can contribute significantly to the mass density. In

our quantitative studies we have therefore used the alpha abundances, measured simultaneously in the solar wind with LASL instrumentation on IMP's 7/8, whenever available. In one case there is also evidence for singly ionized helium.

The UCLA fluxgate magnetometer has been described in detail by Russell (1978). We have utilized the field data with their full time resolution (62.5 to 250 ms) for the determination of boundary locations and for minimum variance analysis (cf. Section 5.3) in 8 of the 11 cases. In the remaining three (5 July, 3 August, and 9 August, 1978) we used averages with 4s spacing. For the quantitative comparisons with the plasma data in Section 5.2, the high resolution magnetic field data were averaged over the precise 9s snapshot times of the 3D plasma measurements.

5. OBSERVATIONS

In this section we will first present and qualitatively discuss examples of ISEE magnetopause crossings, and then apply the tests outlined in Section 3 to a total of 11 cases. Characteristics of these crossings are listed in Tables 1 and 2. The 8 September 1978 magnetopause crossings, although already the subject of paper 1, will be investigated here again, not only to illustrate the method outlined in Section 3, but also because there is additional information, not contained in paper 1, which makes the interpretation of that case in terms of reconnection even stronger.

5.1. Sample Cases

8 September 1978. Figure 2 shows the plasma and magnetic field observations from our instruments on ISEE-1 and -2 for a 36-minute period during

which the satellites moved from the outer magnetosphere through the boundary layer and magnetopause into the magnetosheath. At this time, ISEE-1 was trailing ISEE-2 at a distance (measured along the magnetopause normal) of ~1500 km. The magnetopause, defined as the current layer through which the main transition from terrestrial to interplanetary magnetic field orientation occurs, is identified in this case by the change in B_z from northward to southward (x, y, and z refer to the GSM coordinate system). Earthward of the magnetopause, plasma of magnetosheath origin forms a boundary layer, identified in Fig. 2 by densities above the magnetospheric level of ~ 1 cm^{-3}. In the magnetosheath, the satellites eventually cross the outer separatrix S1 (cf. Fig. 1a). Crossings of this surface are identified by a sudden drop in the density, M_p, of energetic ($\gtrsim$ 13 keV) ions of magnetospheric origin. This feature will be discussed further in Section 5.4.

Owing to motions of the magnetopause, multiple crossings of the various boundary features are observed. The sequence and timing of the magnetopause and separatrix crossings by the two satellites, lead to the schematic picture of radial motions shown in Fig. 3.

Based on the times of the first magnetopause exit (00:44:00 UT for ISEE-1 and 00:41:00 $\pm$ 30s for ISEE-2, with the uncertainty due to a data gap) and a separation distance of 1500 km, a magnetopause speed of 8.5 $\pm$ 1.5 km s^{-1} relative to the spacecraft is derived. Similarly, the times of the final separatrix crossings (00:56:00 UT for ISEE-1, 00:52:40 UT for ISEE-2) yield a speed of 7.5 km s^{-1}. Using 8 km s^{-1}, a total magnetopause thickness of ~ 700 km is inferred, large compared to the gyroradius of a typical magnetosheath (~ 300 eV) ion in a 50 γ field (R_{Li} ~ 50 km). However, the region of most rapid change of $\underline{B}$ is much thinner (~ 80 km). Assuming the same

speed (8 km/s), the boundary layer thickness is estimated at ~1000 km.

Figure 2 shows that the plasma pressure P (defined as in Eq. 11) as well as the magnetic field magnitude B (or pressure $B^2/2\mu_o$) show substantial variations during the magnetopause crossings. However, these variations oppose each other such that the total pressure (not shown here, but see Figure 2 in paper 1) remained very nearly constant. This pressure balance indicates that conditions were sufficiently time-stationary to allow us to proceed with the tests outlined in Section 3.

The important feature to note in Figure 2 is the very large plasma flow speed v_p (up to ~500 km s^{-1}) observed by both spacecraft during each magnetopause encounter and persisting throughout most of the boundary layer. These bulk velocities are directed essentially northward as indicated by the large and positive v_z values. Large increases in plasma flow speeds are the qualitative feature predicted by the tangential momentum balance (cf. Section 3), and such flow enhancements were the principal criterion for the selection of cases to be analyzed further (see Section 5.3).

Figure 2 also shows the intensity of energetic ($\gtrsim$ 13 keV) ions ($\bar{N}_p$ in upper panel), interpreted in Section 5.4 as magnetospheric ions penetrating the magnetopause.

9 August 1978. Figure 4 shows one hour of data from an inbound pass at low latitude near local dusk. It is seen that ISEE-1 started out in the magnetosheath, encountered the magnetopause for an extended time (19:34 UT to 19:53 UT, briefly entering the boundary layer near 19:43 UT), re-entered the magnetosheath, and finally crossed into the magnetosphere around 20:11 UT. The interpretation of the interval between 19:34 UT and 19:53 UT as being the magnetopause follows from a comparison of the

magnetic field components in the L, M, N boundary normal coordinate system (Russell and Elphic, 1979) with those during the complete crossing at ~ 20:10 UT: during the 19:34 UT - 19:35 UT interval B_M only briefly (at 19:43 UT) reached the level characteristic of the magnetosphere after 20:10 UT. The LMN system is such that the positive N-axis points outward along the local magnetopause normal, L lies in the plane defined by N and the z-axis (i.e., it points essentially northward along the magnetopause), and M completes the right-handed system (i.e., it has a negative GSM or GSE y-component). The orientation of N was determined from minimum variance analysis of the magnetic field data (see Table 1). Again large plasma flow speeds occurred throughout the extended magnetopause/boundary layer encounter. However, contrary to the 8 September case (and all others to be discussed in this paper), the z-direction of the flow reversed direction: v_z was directed northward (> 0) in the magnetosheath and turned southward (< 0) at the magnetopause. Such behaviour of the flow velocity is expected for a magnetopause crossing located in the northern hemisphere (external flow northward), but to the south of the separator, as illustrated in Figure 1b. Under these circumstances the tangential magnetic stresses (and consequently the change in flow velocity) are directed southward. An upward tilt of the X-line, as depicted in Figure 1b, is expected for the 9 August 1978 case since the IMF had the necessary positive y-component. Thus, it is plausible that this low latitude crossing could have occurred south of a reconnection line passing through the subsolar point.

3 September 1978. This case is qualitatively very similar to that of 8 September 1978. Figure 5 shows that data for a time interval of the

same length (36 min) as in Figure 2, but the time resolution of the plasma measurements is 4 times less. The actual duration of the magnetopause on 3 September is difficult to determine precisely, since the transition in the magnetic field had a great deal of structure. However, there is clear indication of a boundary layer, lasting at least two minutes. The plasma flow speed was again substantially enhanced during the magnetopause/boundary layer crossing, the flow direction being northward as on 8 September.

28 October 1978. The final example for this qualitative presentation is shown in Figure 6. It is complicated, presumably because of motions of the boundary, leading to a rapid sequence of complete outbound/inbound/outbound magnetopause crossings between 08:21:10 UT and 08:23:20 UT (cf. the B_z panel), and a large number of boundary layer encounters prior to the magnetopause crossings. Increases in plasma flow speed are again substantial, but not as large as in the previous examples.

5.2. Tangential Component Tests

8 September 1978. In paper 1 we analyzed the tangential momentum balance for the 8 September case, using two slightly different methods. First, we compared the total change in tangential plasma flow velocity across the magnetopause with that predicted on the basis of the change in magnetic field. Reasonable agreement was found, both in direction and magnitude (cf. Figure 3 in paper 1). Second, we plotted the measurements of a single component of the velocity during the entire magnetopause encounter versus the corresponding magnetic field measurements. It was found that the slope of the regression line in this plot agreed well

with the predicted slope (cf. Figure 4 in paper 1). However, the analysis in paper 1 did not take into account the effect of the pressure anisotropy factor α (Eq. 4) and did not consider the ISEE-2 data. The present analysis will remove both of these limitations. Also we will use a vector representation of the changes in tangential velocity and magnetic field in the magnetopause in order to provide a better and more detailed illustration of the results of the tangential component test.

Figure 7 shows such vector plots for the 8 September 1978 crossing, for both ISEE-1 and -2. Each vector in these figures represents the measured change in tangential velocity, $(\underline{v}_{2t} - \underline{v}_{1t}) = \Delta\underline{v}_t^{obs}$, between a fixed point in the magnetosheath (subscript 1) and a point in the magnetopause or boundary layer (subscript 2). The magnitude of each vector is normalized by the corresponding theoretically predicted change $|\Delta\underline{v}_t^{th}|$, given by Eq. 7, and calculated using measured magnetic fields, mass densities and pressure anisotropies. In reality, the direction of each vector $\Delta\underline{v}_t^{th}$ is also different for different points in the magnetopause. To facilitate comparison between $\Delta\underline{v}_t^{obs}$ and $\Delta\underline{v}_t^{th}$ we have rotated each $\Delta\underline{v}_t$ pair about the magnetopause normal, maintaining the actual angle between the two vectors, until $\Delta\underline{v}_t^{th}$ (given by Eq. 7, using the positive sign) is horizontal and points to the right in the diagram.

Thus, in Figure 7 all of the $\underline{v}_t^{th}$ vectors are represented by a single horizontal vector of unit magnitude. Agreement between the observed and predicted directions of $\Delta\underline{v}_t$ (test Ia) appears as precise alignment of the measured vectors with the horizontal. The amount of disagreement is directly shown by the angle between these vectors and the horizontal. In the reconnection model, vectors which point along the horizontal to the right correspond to crossings north of the separator

($B_n < 0$) ; those pointing to the left correspond to crossings south of that line ($B_n > 0$) and it is expected that for a given event the vectors should point either consistently to the right or consistently to the left (test Ib). The normalization of the length of the vectors is such that their tips will lie on the unit circle if measured and predicted magnitudes of $\Delta \underline{v}_t$ agree precisely (test Ic).

The reference point in the magnetosheath (subscript 1 in Eq. 7) was chosen close to the magnetopause with the provision that the plasma density and velocity, as well as all magnetic field components had assumed fairly constant levels representative of magnetosheath conditions. The relevant quantities are listed in Table 2.

The measurements within the magnetopause and boundary layer (index 2 in the equations) were subjected to a number of rigorous selection criteria designed to reduce the number of points likely to be affected by substantial measurement errors. These criteria are described in the Appendix. In the case of 8 September, this procedure led to the exclusion of approximately two thirds of the measurements. In particular no points were used during the most rapid field variation in the first ISEE-1 magnetopause crossing. For the remaining data, the vectors $\Delta \underline{v}_t^{obs}$ were constructed from the measured 3D velocities, using a magnetopause normal (cf. Table 1) obtained from minimum variance analysis (see Section 5.3).

The mass densities, ρ , the tangential components of the magnetic field, $\underline{B}_t$, as well as the anisotropy factor α_1 , needed to calculate the theoretical value of the tangential velocity change according to Eq. 7, were obtained as described in Section 4. For the determination of ρ we used the alpha/proton number density ratio of 2.5%, measured simultaneously in the solar wind by the LASL instrument on IMP-7. (As discussed in

Section 5.4, there is also evidence for some ionospheric helium during the crossing. Its effect on the mass density, however, would be rather small.) The pressure anisotropy was found to be $\alpha_1 \approx -0.2$, i.e. $p_\perp > p_\parallel$. The resulting correction to $\Delta \underline{v}_t^{th}$, being proportional to $(1 - \alpha_1)^{1/2}$, is rather small (~ 10%). Thus, the omission of the pressure anisotropy in paper 1 was justified.

Figure 7 demonstrates that for 8 September 1978 (a) there is, on the average, fairly good alignment (deviations < 25^o) of the vectors with the horizontal indicating that $B_n \neq 0$ (test Ia); (b) all the vectors point to the right, i.e. $\Delta \underline{v}_t$ and $\Delta \underline{B}_t/\rho$ are parallel, indicating a consistently negative B_n , i.e. a crossing north of the separator as expected at this location (25.9^o N, 11.41 h LT) (test Ib); (c) the magnitudes of several of the vectors are near the theoretical prediction (test Ic), although on average their magnitude is only 0.8 of the theoretical value.

In order to understand the origin of the scatter of the vectors in Figure 7 around the theoretical prediction, several effects must be considered. First, there are errors in determining the flow velocity. As shown in Section 4, these errors typically range up to ~ 20% (i.e. 100 km s^{-1} for the present case) and are such that the derived flow velocities tend to be underestimated, thus explaining, at least in part, the fact that the majority of the vectors in Figure 7 fall short of the unit circle. Second, the measured flow velocities include finite gyroradius effects such as pressure gradient drifts, which for reasonable pressure gradients can easily amount to 50 km s^{-1} and which are not incorporated in Eq. (3) or (7). As these drifts are directed perpendicular to the magnetic field, their effect will mainly show up in angular

deviations. Third, the presence of ionospheric ions with large mass (e.g. oxygen) within the magnetopause and boundary layer would increase the mass densities ρ_2 and thus systematically increase the magnitude (and change the direction) of the normalized vectors. Fourth, there are errors in the pressure anisotropy factor α_1. However, α_1 only enters as the square root $(1 - \alpha)^{1/2}$, and it only affects the magnitude, not the direction, of the vectors. Fifth, some of the assumptions in the theoretical model, in particular those concerning the one-dimensional time-stationary structure of the magnetopause are unlikely to be precisely valid and could affect the comparison. It should be noted that errors up to ~ 30^{o} in the magnetopause normal direction do not significantly affect the comparison.

Because of these various error sources, we believe that the deviations in Figure 7 of the measured velocity changes from the theoretical ones are sufficiently small to permit of the conclusion that the data are compatible with the reconnection hypothesis.

9 August 1978. In Section 5.1 we noted that the behaviour of the flow velocity for this low latitude crossing was qualitatively consistent with a crossing southward of the separator. Figure 8 shows the result of the quantitative analysis, in the format discussed above. In computing the mass densities ρ, we used a measured alpha particle abundance of 1.5%. The pressure anisotropy factor α_1 was so small (- 0.05) that its effect could be neglected. Figure 8 shows that there is fairly large scatter in the direction of the vectors, and that angles with the horizontal of up to ~40^{o} occur. However, the average of the magnitude of the angles was only 24^{o}. In view of the uncertainties in the analysis, discussed

above, this may be regarded as reasonable agreement with the predicted direction (test Ia). Note that contrary to the 8 September case, the vectors now consistently point to the left, indicating a negative sign in Eq. 7, i.e. $B_n > 0$ or a crossing south of the separator (test Ib). The agreement between measured and predicted magnitudes of the vectors is again reasonably good (test Ic). The average magnitude of the measured vectors in Figure 7 is about 90% of the predicted value. Because flow elevation angles in this case are small, no systematic underestimate of the flow velocities is expected. Lengths greater than unity, as in Figure 8, could be the result of time variations, for example, in the magnetosheath reference level.

Other Cases. The result of the analysis of 9 additional crossings is presented in Figure 9. These cases (and the ones already presented) were discovered in a systematic search for substantial flow speed increases in all dayside magnetopause crossing by ISEE between October 1977 and the end of 1978. The figure includes one 1979 case, although no systematic search of the 1979 crossings has yet been undertaken. Figure 9 includes the crossings of 3 September 1978 and 28 October 1978 shown in Figures 5 and 6, respectively. Relevant characteristics of all these crossings are listed in Tables 1 and 2. Whenever simultaneous measurements of the solar wind alpha abundance were not available, we used a value of 5%. The pressure anisotropy factors were in the range $-0.25 < \alpha_1 < 0$ in all cases. The magnetopause normals used in the analysis were based on the minimum variance technique, if successful. Otherwise a model normal was chosen based on the average shape of the magnetopause (Fairfield, 1971). The normals are listed in Table 1, with an indication of how they were derived. It should be remembered that the tangential component tests do not

require an accurate knowledge of the normal direction.

The various cases in Figure 9 differ considerably in the number of measurements for which a comparison could be made. Cases with very few points represent either cases with brief magnetopause/boundary layer crossings, or those where many points did not meet the selection criteria (cf. Appendix).

The overall impression from Figure 9 is that, given the uncertainties discussed earlier, there is reasonable agreement between measurements and predictions , with respect to the alignment of the vectors with the horizontal as well as their magnitude. In all nine cases the vectors point consistently to the right, indicating that the observations were made north of the separator ($B_n < 0$) . Given the location of these crossings in the northern hemisphere, this latter result is consistent with our expectations.

Summary. For each of the 11 cases presented we have averaged the individual vectors (shown in Figs. 7 to 9) by first decomposing them into the components parallel and perpendicular to the predicted directions and then averaging these components. The result is shown in Figure 10, where each crossing is now represented by a single normalized vector. (For simplicity, we have reversed the direction of the 9 August 1978 vector and shown it as a dashed line.) The actual magnitude of the maximum velocity increase is given in Table 2. It ranged from 128 - 462 km s^{-1}. Figure 10 demonstrates that on average the agreement between measurements and predictions is quite good, considering the number of uncertainties that enter into the comparison.

5.3. Normal Component Tests

8 September 1978. In paper 1 the normal vector and normal field component for the principal ISEE-1 crossing were given as $\underline{n}' = (0.80, -0.40, 0.45)$ (in spacecraft coordinates) and $B'_n = (-5.4 \pm 2.9)$ nT . Those results were obtained by use of the minimum variance technique on 12s magnetic field averages with two thirds overlap. We have repeated the analysis using the full resolution (62.5 ms) data, the result being $\underline{n}'' = (0.80, -0.44, 0.42)$ and $B''_n = (-9.2 \pm 1.9$ nT) . In view of the size of the error estimates (obtained as in Sonnerup, 1971), the two B_n values are not inconsistent with each other and we feel confident in concluding that B_n was negative for this crossing. This is in agreement with the sign inferred from the tangential component test (Ib) so that this crossing also passes the first part of the normal component test (IIa).

For the partial ISEE-1 crossing no reliable normal vector determination was possible. Using the vector $\underline{n}''$ given above and the field vectors selected for the tangential test, one finds B_n values ranging from -2.7 to -11.7 nT with an average of -7.2 nT for this crossing. The ISEE-2 magnetopause crossing contains a large data gap so that again no reliable normal vector could be found. Using the vector $\underline{n}''$ and the field data employed in the tangential test, B_n for this crossing ranged from -6.1 to -16.7 nT with an average of -11.0 nT. These results are in agreement with our conclusion that B_n was negative for the 8 September event.

Turning now to the normal flow component, the data for the principal ISEE-1 crossing in Figure 3 of paper 1 indicated $v_n = (-17 \pm 11)$ km s^{-1} (the uncertainty being the standard deviation of the mean), based on the normal vector $\underline{n}'$. If only the data points selected for the tangential test are used, with the new vector $\underline{n}''$, then $v_n = (2 \pm 14)$ km s^{-1} .

Similarly, for the partial ISEE-1 crossing $\underline{v}_n = (-34 \pm 6)$ km s^{-1} and for the ISEE-2 crossing $\underline{v}_n = (-54 \pm 8)$ km s^{-1}. We have estimated the magnetopause speed to be $U_n = -8$ km s^{-1} for the principal ISEE-1 and for the ISEE-2 crossing, while for the partial ISEE-1 crossing, where the magnetopause reversed its direction of motion, the appropriate value is $U_n \simeq 0$. Thus, the flow speed $(v_n - U_n)$ across the magnetopause corresponding to the four v_n values given above is -9, +10, -34, and -46 km s^{-1}, respectively. The prepondèrance of the evidence is that $(v_n - U_n)$ was negative so that the 8 September event passes the second part of the normal component test (IIb). This statement implies only that the normal velocity results are compatible with the conclusion that an inflow occurred across the magnetopause, not that they prove the existence of such an inflow.

The flow speed across the magnetopause predicted by Eq. 5, with $B_n = -9.2$ nT and the density, anisotropy and alpha particle abundance given in Table 2, is $(v_n - U_n) = -55$ km/s. Given the large uncertainties, this result is not incompatible with the measured values given above. In this sense, the 8 September case also passes test IIc. The comparison with Eq. 5 suggests that a somewhat smaller B_n magnitude, perhaps the original $B_n = -5.4$ nT, may provide better agreement between theory and observations.

9 August 1978. From the analysis of the tangential components of the plasma velocity and magnetic field in Section 5.3, we determined that the normal components of the magnetic field for the 9 August case had to be positive, $B_n > 0$, i.e. that the crossing was located south of the separator (cf. Figure 1b). Unfortunately, the situation on this occasion is complicated by the fact that the magnetopause crossing, where the large

plasma flow speeds were observed (19:34 UT - 19:53 UT; cf. Figure 4), was not complete. Therefore, no reliable normal direction could be determined. When using the normal determined from minimum variance analysis of the final magnetopause crossing at 20:10 UT, no significant B_n and v_n are obtained for the first entry near 19:34 UT. However, for the period near 19:53 UT one obtains $B_n = (2.2 \pm 1.0)$ nT and $v_n = (-25 \pm 8)$ km s^{-1}, where the uncertainties are the standard deviations of the mean values. B_n has the expected sign, and therefore passes test IIa. The topology test, to be discussed in Section 5.4, also supports the conclusion $B_n > 0$. The magnetopause speed, U_n, and consequently $(v_n - U_n)$, could not be determined because the two satellites were very closely spaced. However, examination of Figure 4 suggests that U_n was small at 19:53 UT. Thus, it is likely that $(v_n - U_n)$ was negative as required by test IIb.

Other Cases. The minimum variance technique was also applied to the remaining 9 cases. In two of these the technique was unsuccessful and did not provide a reliable normal direction (cf. Table 1). The average field component along the model normal was negative for both cases. In those 7 cases where a reasonable normal was obtained, the corresponding B_n was nevertheless not well determined for the individual cases. However, in all but one of them (4 November, 1978) the average value of B_n for each crossing had a sign consistent with that derived from the tangential component test (Section 5.2). For the 4 November case, the average B_n had the wrong sign but its magnitude was less than the error estimate. Thus, there is no direct conflict between the results of the tangential and the normal component test in this case either. Moreover, the energetic particle analysis (Section 5.4) confirms the sign of B_n derived from the

tangential component test. Averaging over the seven crossings, we obtained $B_n = (-3.5 \pm 1.1)$ nT , where the error is the standard deviation of the mean. Thus, in an average sense, these 7 cases also pass test IIa.

Averaging the measured normal plasma velocities for the same 7 cases, one obtains a value $v_n = (-37 \pm 5)$ km s^{-1} . The sign is that expected for an inward plasma flow across the magnetopause (test IIb). Moreover, the magnitude is consistent with the predicted one. Using $B_n = -3.5$ nT and an average plasma density of 20 cm^{-3}, equation 5 (neglecting the effects of pressure anisotropy and alpha particles) predicts $(v_n - U_n) = -17$ km s^{-1}. Since our measured average normal flow speed is $v_n = -37$ km s^{-1} , this result indicates an average magnetopause velocity, $U_n \approx -20$ km s^{-1} . Because all 7 crossings occurred on outbound orbits, the magnetopause velocity should indeed be inward, i.e. $U_n < 0$; the predicted value is also reasonable.

5.4. Topology Test

In this section we will discuss inferences concerning the magnetic field topology obtained by using energetic ions of magnetospheric origin as field line tracers. It is not our intention to give a full discussion of the energetic particle escape from the magnetosphere. In particular, the problem of the continuous supply (e.g. Scholer, 1981) of these particles is ignored. We only ask whether the energetic ion behaviour is consistent with the conclusions on the field topology reached in previous sections. We also have neglected electrons, because their intensities and anisotropies are more variable.

8 September 1978. Figure 11 shows a time sequence of ion energy spectra from ISEE-1 covering the time period between 00:40 UT and 01:00 UT. The figure demonstrates that a separate high-energy component ($E \gtrsim 5$ keV) existed, which lasted well into the magnetosheath where, at the point marked S in the figure (~ 00:56 UT), these ion fluxes suddenly dropped. This same fact is also apparent in Figure 2, which shows the density, $\bar{N}_p$, of protons $\gtrsim 13$ keV as a function of time. The purpose of showing the spectra is to demonstrate that the energetic ions represent a separate population and not just the high-energy tail of a hot magnetosheath ion distribution. The hypothesis that these ions are of magnetospheric origin is supported by the fact that their intensity does not change across the magnetopause and boundary layer.

An important property of the energetic ion population is its pronounced anisotropy. This is demonstrated in Figure 12, which shows a relief plot of the entire two-dimensional velocity distribution at 00:52:00 UT, as measured by ISEE-1, together with the projected magnetic field direction. The distribution shows 4 separate ion populations, ranging in velocity from ~ 115 up to ~2500 km s^{-1}. Peak number 1 represents the shocked solar wind flowing towards and along the magnetopause. (Because we are using count-rates as the intensity measure, rather than phase space densities, this peak is underemphasized in Fig. 12.) The significance of peaks 2 and 3 will be discussed below. The energetic magnetospheric ions referred to above are readily discernible as the crescent-shaped feature at the highest velocities (population 4 in Fig. 12). These ions are seen to move predominantly in a direction antiparallel to the magnetic field. This is exactly what is expected if these particles had leaked out of the magnetosphere along reconnected field lines north of the separator where

$B_n < 0$, as illustrated by Figure 1b. Thus the energetic particle population on 8 September passes test IIIa, i.e. it supports the earlier conclusion concerning existence and sign of B_n . The same conclusion has been drawn recently by Scholer et al. (1981) for this crossing, on the basis of energetic particle data from a different experiment onboard ISEE-1.

Another feature of the energetic particles is their sudden disappearance near 00:56 UT in the ISEE-1 record (the point S in Figures 2 and 11), which we interprete as the crossing of the outer separatrix S1. From Figure 1a it is evident that the total magnetic flux between the magnetopause and the outer separatrix must cross the magnetopause between the location of the satellite crossing and the separator. Assuming B_n to be known and constant, the distance Δl along the magnetopause from the satellite to the X-line is thus estimated as $\Delta l = \frac{B}{B_n} \Delta s$ where Δs is the distance between the magnetopause and the outer separatrix. As it happens, ISEE-2 was crossing the outer separatrix almost precisely when ISEE-1 exited the magnetopause. This is illustrated in Figure 3. The evidence is shown in Figure 2, where the dashed lines in the ISEE-2 graph, which mark the magnetopause exit times of ISEE-1, twice nearly coincide with the times ISEE-2 experienced the sharp drops in $\bar{N}_p$, identified as separatrix crossings. Accordingly, $\Delta s \sim 1500$ km , the separation distance of the two spacecraft along the magnetopause normal. Using $B_n = -5.4$ nT and -9.2 nT and $B \sim 54\ \gamma$ (see Table 2), one obtains $\Delta l \sim 2.4\ R_E$ and $1.4\ R_E$, respectively. Admittedly, these determinations of Δl can only be regarded as crude estimates. But even if one allows for an uncertainty of a factor of two, it is clear that the X-line could not have been located in the southern polar cusp region. On the other hand, the derived distances are consistent with a location near the equatorial plane, $\sim 3.5\ R_E$ south of the satellites.

A final point concerns the identification of peaks 2 and 3 in the distribution of Figure 12. We interprete the former as the result of reflection of the shocked solar wind plasma (peak 1) at the magnetopause, which causes a velocity change given by Eq. 8. Using the values in Table 2, one derives a velocity of the reflected ions of about 500 km s^{-1} directed essentially antiparallel to the magnetic field, in good agreement with the observations. The density contained in peak 2 is about 20% of the total density. Thus magnetopause reflection is rather efficient in this case.

The significance of the reflected ions is threefold: First, they trace out the field topology in much the same way as the leaking magnetospheric ions do. In particular, they should terminate at or near the outer separatrix, and that is indeed what is observed (cf. Figure 11). Thus the reflected ions support our identification of the outer boundary of magnetospheric ions as the separatrix. Second, their energization during the reflection provides additional evidence for the presence of a tangential electric field E_z at the magnetopause. Third, along with ions leaking out from the magnetosphere, they constitute an ion heat flow which carries energy away from the magnetopause.

Peak 3, which is very pronounced in Figure 12, but appears mostly as a shoulder in the spectra of Fig. 11, is interpreted as singly-ionized helium, presumably of ionospheric origin. At about this time the ion mass spectrometer experiment on ISEE-1 observed He^+ with a density of ~ 0.8 cm^{-3} and a velocity of ~ 300 km s^{-1} antiparallel to the magnetic field (W.K. Peterson, private communication). These numbers are consistent with the location and intensity of peak 3 in Figure 12. Note that in constructing Figure 12, all ions were assumed to be protons. With the

proper mass, peak 3 would have appeared at half the velocity, and its contribution to the ion number density would have been twice as large. But compared to the total number density, the He^+ contribution is rather insignificant: Even in terms of the mass density needed in the calculations of Section 5.2, it is only of the same order as that of the solar wind alphas.

9 August 1978. In Section 5.2 we inferred on the basis of the tangential component test that this crossing occurred south of the reconnection line. Magnetospheric particles leaking out along reconnected field lines should then move preferentially parallel rather than antiparallel to the external magnetic field (test IIIa). Figure 13 shows a measured distribution outside the magnetopause on 9 August, in the same format as Figure 12. Again the magnetospheric ions appear as a separate component and they do indeed move parallel to the magnetic field. Contrary to the 8 September case, there is no clear indication of magnetopause reflection.

Other Cases. We have examined the other 9 cases for evidence of leaking energetic magnetospheric particles. As a criterion we not only required the presence of ions with energies $\gtrsim$ 5 keV, but also that they appeared as a separate component, i.e. that there was a change in spectral slope such as shown in Figure 11. Thus energetic ions which just constitute the high-energy tail of a hot magnetosheath distribution were excluded. Four of the nine cases met this criterion (see Table 2). Of the five that did not, one showed no energetic ions above our sensitivity threshold, and four showed no clear change in spectral slope within our energy range. Note that the existence of magnetospheric ions outside the magnetopause

cannot be excluded even in these five cases. Both limited sensitivity and energy range could be responsible for our failure to detect them.

Of the four cases that met our criterion (3 August, 5 September, and 4 November, 1978; 11 September 1979), all showed the energetic ions moving antiparallel to the external magnetic field (test IIIa). This can be verified by comparing the magnetic field direction, ϕ_{B1}, with the energetic ion streaming direction, ϕ, in Table 2. This result is in accordance with the conclusion $B_n < 0$ reached for these cases on the basis of the tangential component test. No clear indication of reflected ions was detected.

5.5. Tangential Electric Field

As discussed in Sections 2 and 3 and illustrated in Figure 1, the reconnection process implies the existence of an electric field E_t tangential to the magnetopause. Once the sign of B_n is known, the direction of this field can be determined rather easily from the plasma and magnetic field data because only tangential components are involved (Eq. 9). The field direction is of interest when compared with that of the magnetopause current, because $\underline{E}_t \cdot \underline{I}$ measures the electromagnetic power converted at the magnetopause. Figure 14 shows the result of this comparison for all 11 cases. For each crossing, we first calculated the average $\underline{B}_t/B_n$ from Eq. 9. Using the sign of B_n as derived from the tangential component tests (Section 5.2), we then obtained $E_t/|B_n|$. The magnetopause current $\underline{I}$ was calculated from the measured field change, $\Delta\underline{B}$, across the magnetopause. Figure 14 illustrates that although the angle between $\underline{E}_t$ and $\underline{I}$ varies over a large range, $\underline{E}_t \cdot \underline{I}$ is positive in all cases.

The magnitude, E_t , of the tangential electric field is more difficult to obtain from our measurements because, according to Eq. 9, it is proportional to B_n . For the 8 September 1978 case, where B_n is reasonably well determined, we derived a value $E_t \sim 1.8$ mV/m in paper 1, based on $B_n = -5.4$ nT and data from the principal crossing of ISEE-1 only. Using all the ISEE-1 and -2 data which passed the acceptance criteria (see Appendix) the values of E_t for this case were 1.7 mV/m and 2.8 mV/m, corresponding to $B_n = -5.4$ nT and -9.2 nT , respectively.

As pointed out already, B_n is not well determined for the remainder of the cases. However, an estimate of E_t can still be obtained by using the average $B_n = -3.5$ nT given in Section 5.3 for 7 of the cases, and the average E_t/B_n for the same cases. This procedure yields an average E_t of ≈ 0.8 mV/m.

The magnitudes of the tangential electric fields thus inferred are of the same order as that determined directly from the electric field measurements for an ISEE magnetopause crossing on 20 November 1977 (Mozer et al., 1979). However, we did not observe significant plasma flow enhancements during this crossing.

6. SUMMARY AND DISCUSSION

We have examined eleven crossings of the dayside magnetopause in the northern hemisphere by the ISEE spacecraft. The locations of these crossings are given in Table 1. They were selected because of large plasma flow speeds observed in the magnetopause and boundary layer. It has been the purpose of our examination to test the hypothesis that these large speeds were the result of the plasma acceleration intrinsic to the magnetic field reconnection process. Our conclusions are as follows:

(1) The direction and magnitude of the difference between the plasma velocity measured at a reference point in the magnetosheath and those measured at individual points in the magnetopause or boundary layer are in reasonably good agreement with predictions from the reconnection model. For 10 of the crossings, the direction of the plasma acceleration was that associated with a consistently negative (inward) magnetic field component, B_n , normal to the magnetopause, as expected in the northern hemisphere of the standard reconnection model in which the magnetic separator passes through the subsolar point. The remaining case (August 9, 1978) displayed acceleration corresponding to $B_n > 0$. This case too is compatible with the standard model: the crossing occurred on the post-noon side near the equatorial plane and the magnetosheath field had a positive B_y component, presumably causing the X-line to deviate northward from the equatorial plane in the post-noon sector. For the eleven cases, the angle change across the magnetopause of the magnetic field vector ranged from 88^o to 170^o; the maximum velocity change was in the range 128 - 462 km/s.

(2) The normal magnetic field components determined from minimum variance analysis of the magnetic data had large uncertainties for most of the crossings. However, except for one case (4 November, 1978) the average B_n thus determined had the same sign as that predicted from the plasma results. For the 4 November case, B_n was less than the uncertainty in B_n , and the plasma prediction of the sign of B_n is probably the correct one. For the 8 September 1978 case the determination was reasonably good and yielded B_n values in the range -5 to -9 nT. The composite average for the 7 other cases (all north of the X-line), for which a minimum variance normal was obtained, was $B_n = -3.5 \pm 1.1$ nT .

(3) In 6 of the 11 cases, a distinct population of energetic (E > 5 keV)

particles was found in the magnetosheath just outside the magnetopause. We find the evidence to be strong that this population represents magnetospheric particles that leaked across the magnetopause as a result of the presence of a nonvanishing normal magnetic field component there (see also Scholer et al., 1981). In all cases where the inferred B_n was negative, this energetic particle distribution showed a strong anisotropy indicating streaming antiparallel to the magnetic field. For the one case with an inferred positive B_n value (9 August, 1978), the anisotropy was also strong but indicated flow parallel to the field instead. These results are again in agreement with expectations for the standard reconnection model. The field topology in that model is such that the leaking energetic particles should terminate at (or slightly inside) the outer separatrix surface. A well-defined termination is indeed observed in most cases, and in one case (8 September, 1978) the distance between separatrix and magnetopause could be determined to be ~ 1500 km. For this case, we estimated the distance along the magnetopause from the spacecraft southward to the X-line to be 1.4 - 2.4 R_E . This result is compatible with an X-line located in the vicinity of the equatorial plane (near the noon meridian) but not in the southern polar cusp.

(4) In one case (8 September, 1978), the plasma distributions in the magnetosheath, adjacent to the magnetopause, also displayed a pronounced peak at an energy of ~ 1 keV, produced by particles streaming away from the magnetopause in a direction approximately antiparallel to the magnetic field. It is likely that these are magnetosheath particles that have been reflected at the magnetopause and in the process have been energized by the tangential electric field in the same manner as particles transmitted through the magnetopause to form the boundary layer. The situation is

essentially identical to that at the earth's bow shock where incident solar wind ions are occasionally reflected and energized by the solar wind electric field (Sonnerup, 1969; Paschmann et al., 1980). This type of reflection requires $B_n \neq 0$. The observed energy of the reflected ions is in good agreement with the theoretically predicted value. The reflected particles also constitute a substantial ion heat flux away from the magnetopause.

(5) On the strength of the evidence summarized above, we tentatively accepted the validity of the reconnection hypothesis, and proceeded to estimate the electric field component $\underline{E}_t$ tangential to the magnetopause. This field is proportional to B_n and our estimate of the field magnitude is therefore no better than that of B_n. We find that, for an individual crossing, the calculated vectors $\underline{E}_t/|B_n|$ scatter considerably, both in magnitude and direction, whereas Maxwell's equations require $\underline{E}_t/|B_n|$ to remain constant across a time-independent one-dimensional magnetopause. Gradient drift effects, not included in the calculation, may account for some of the discrepancy but it seems likely that two and three-dimensional fluctuations also play a major role. The average $\underline{E}_t/|B_n|$ vector for an individual crossing may form a substantial angle with the total magnetopause current $\underline{I}$, as a result of plasma motion and magnetic fields along it, but the composite average for all the crossings is nearly along $\underline{I}$. For the 8 September case, E_t = 1.7 - 2.8 mV/m. For the 7 other cases north of the X-line for which a reliable minimum variance normal was obtained, the average E_t is 0.8 mV/m.

The ratio $B_n/B = v_n/v_A = M_{An}$ is a convenient (but imprecise, due to the unknown separator orientation) nondimensional measure of the reconnection rate. For the 8 September event this Alfvén-Mach number was

$M_{An} \approx 0.10 - 0.17$; for the other 7 cases, referred to above, the average was $M_{An} \approx 0.10$. These values are in the range predicted by Levy et al. (1964).

We have also examined the tangential momentum balance for a few selected crossings in which no substantial increase in plasma flow speed was seen at the magnetopause, including one case, at substantial northern latitude, where the direction of the plasma flow vector was reversed across the magnetopause (a possible signature of northern cusp reconnection). In these cases, no agreement was found with the tangential momentum balance equations in Section 3. However, no systematic study of all ISEE magnetopause crossings has been undertaken so that firm statistical information is not available concerning the frequency of occurrence of cases that obey the tangential momentum balance equations. In particular, we are not in a position to exclude the possibility that cusp reconnection takes place occasionally.

It is noteworthy that no acceleration events were found during the first coverage of the subsolar region by the ISEE spacecraft after their launch in October 1977. It is tempting to speculate that the sudden appearance of events in the summer and fall of 1978 is related to the sharply rising sunspot activity at that time. However, we have been unable to identify any single dimensionless group such as the magnetosheath plasma β value (see Table 2) or the Alfvēn-Mach number that correlates with the presence and absence of accelerated plasma at the magnetopause. However, there is a striking relation with the sign of the y-component of the magnetosheath magnetic field. As is evident from Table 2, the azimuth angle ϕ_{B1} of the field varied between 33^{o} and 137^{o}, i.e. $B_y > 0$ for all 11 cases.

Preliminary analysis of magnetopause crossings for which no high-speed plasmas were observed, indicates that these occurred for both signs of B_y .

In closing, we comment briefly on the question whether the evidence for reconnection presented here should be considered "incontrovertible". In a strict sense, incontrovertible evidence consists of a direct reliable measurement of an electric field along a separator, since that is the basic definition of reconnection. In practice, however, it is very hard to identify an encounter with an X-line unambiguously and indeed such an encounter is in itself an unlikely event (although one potential case has in fact been reported (Sonnerup, 1971)). One must therefore rely on indirect evidence such as $B_n \neq 0$, the presence of plasma jets at the magnetopause, and topological evidence provided by leaking or reflected particles. Direct measurement of a nonvanishing $\underline{E}_t$, as reported by Mozer et al. (1979), is, of course, also extremely important. Individually, such observations are not convincing; collectively they may become very persuasive, in particular when quantitative agreement between theory and observations is found, as in the cases presented here. But they are not absolutely incontrovertible. For example, the presence of a nonvanishing $\underline{E}_t$ at a position away from the X-line does not by absolute necessity imply that an electric field is or has been present along such a line (or for that part that the line itself exists). Only in simple, steady-state plane geometries, as in Fig. 1a, does an $\underline{E}_t$ anywhere imply an $\underline{E}_t$ along the X-line.

Even though we cannot exclude other explanations entirely, the possibility seems very remote that the observations reported here do not constitute a manifestation of reconnection. Thus they should effectively

remove one of the last major obstacles to the acceptance of magnetopause reconnection as an important magnetopause process, namely the lack of observations of plasma accelerated by the $I \times B_n$ force. The fact that dramatic events of the type presented here appear to be relatively rare should not be construed to mean that magnetopause reconnection itself is rare - the indirect evidence to the contrary is very strong, not to say overwhelming - but only that reconnection in a quasi-steady state over a broad segment of the dayside magnetopause is rare. In retrospect, the widespread belief that the Levy-Petschek-Siscoe (1964) model would apply most of the time over most of the dayside magnetopause was perhaps an unrealistic one. The situation may be more like that of a turbulent boundary layer in ordinary fluid mechanics: the probability of observing the classical turbulent velocity profile everywhere, or indeed anywhere, in a boundary layer at any chosen instant is essentially zero yet the average profile is highly reproducible and extremely useful. In the same way, the Levy-Petschek-Siscoe model may usually only emerge as a time average in that sense, we have been fortunate to find individual events that agree approximately with this simple model.

In the case of a turbulent boundary layer, one must develop a detailed understanding of the nature of the velocity fluctuations in order to properly evaluate the turbulent transport properties across the layer. In the same way, we must develop a far better understanding of flux transfer events (Russell and Elphic, 1979) and other turbulent signatures of the magnetopause before we can begin to evaluate the contribution of patchy time-dependent reconnection to the transfer of mass, momentum, and energy across the magnetopause.

APPENDIX

This Appendix describes the criteria used in selecting the plasma data for the tests in Section 5.2.

First, we removed all measurements for which $\rho_2/\rho_1 \leq 0.5$ to ensure that the test was applied to plasma of magnetosheath origin rather than to purely or predominantly magnetospheric plasma. Second, we analyzed only those measurements showing significant bulk speed increases over the magnetosheath level ($v_2 - v_1 > 0.5\ v_1$) . Third, we discarded measurements for which the instrument response was essentially limited to the highest elevation channel, in which case the moments become unreliable (see Section 4). Fourth, in the same spirit, we discarded all measurements where the computed bulk velocity had an elevation angle with the ecliptic plane of $|\Lambda_p| \geq 55^o$ (see Section 4). The fifth selection criterion concerns the behaviour of the magnetic field during the 9s period in which the 3D distribution function of the plasma is being measured. If the magnetic field varies strongly during this interval, the plasma measurements are likely to be time-aliased. As a rejection criterion we used

$$\epsilon \equiv \frac{(\delta B_1^{\,2} + \delta B_2^{\,2})^{1/2}}{|\underline{B}_2 - \underline{B}_1|} \geq 0.45$$

where $\underline{B}_1$ and $\underline{B}_2$ are the magnetic field vectors, obtained by averaging the original field data precisely over the 9s interval of the plasma measurements; δB_1 and δB_2 are the standard deviations of the magnetic field magnitude in the same interval. The above condition rejects all measurements where the fluctuation in the difference vector is larger than 45% of the difference itself. The value of the threshold is somewhat

arbitrary. We chose $\varepsilon = 0.45$ because the distribution of ε values for the entire set of plasma measurements in the 11 crossings had a local minimum there.

Finally, if the densities, measured with higher time resolution by our 2D instruments, indicated variations by more than 50% during the 9s snapshot time of the 3D measurements, the data points were also discarded.

ACKNOWLEDGEMENT

The Max-Planck-Institut portions of this work were supported by the Bundesministerium für Forschung und Technologie under grant 01 OI O 27-ZA/WF/WRK 275:4. Los Alamos portions were done under the auspices of the US Department of Energy with NASA support under S-50864A. Work at UCLA was supported under NASA contract NAS-5-20064, that at Dartmouth by an ISEE Guest Investigatorship (NASA grant NSG 5348) and by the National Science Foundation, Atmospheric Science Division, under grant ATM-7920277.

REFERENCES

Alfvén, H., On frozen-in field lines and field-line reconnection, J. Geophys. Res., 81, 4019-4021, 1976.

Axford, W.I., Magnetospheric convection, Rev. Geophys., 7, 421-459, 1969.

Bame, S.J., J.R. Asbridge, H.E. Felthauser, J.P. Glore, G. Paschmann, P. Hemmerich, K. Lehmann, and H. Rosenbauer, ISEE-1 and ISEE-2 fast plasma experiment and the ISEE-1 solar wind experiment, IEEE Transact. Geosci. Electron., GE-16, 216-220, 1978.

Cowley, S.W.H., Comments on the merging of nonantiparallel magnetic fields, J. Geophys. Res., 81, 3455-3458, 1976.

Crooker, N.U., Antiparallel merging, the half-wave rectifier response of the magnetosphere, and convection, in: Magnetospheric Boundary Layers (B. Battrick, ed.),pp. 343-348, Paris: ESA SP-148, 1979.

Dungey, J.W., Interplanetary magnetic fields and the auroral zones, Phys. Rev. Lett., 6, 47-48, 1961.

Elphic, R.C., and C.T. Russell, ISEE-1 and -2 magnetometer observations of the magnetopause, in: Magnetospheric Boundary Layers (B. Battrick, ed.), pp. 43-50, Paris: ESA SP-148, 1979.

Fairfield, D.H., Average and unusual locations of the earth's magnetopause and bow shock, J. Geophys. Res., 76, 6700-6716, 1971.

Gonzalez, W.D., and F.S. Mozer, A quantitative model for the potential resulting from reconnection with an arbitrary interplanetary magnetic field, J. Geophys. Res., 79, 4186-4196, 1974.

Haerendel, G., G. Paschmann, N. Sckopke, H. Rosenbauer, and P.C. Hedgecock, The front side boundary layer of the magnetosphere and the problem of reconnection, J. Geophys. Res., 83, 3195-3116, 1978.

Heikkila, W.J., Is there an electrostatic field tangential to the day-side magnetopause and neutral line? Geophys. Res. Lett.,2, 154-157, 1975.

Hudson, P.D., Discontinuities in an anisotropic plasma and their identification in the solar wind, Planet. Space Sci., 18, 1611-1622, 1970.

Hudson, P.D., Rotational discontinuities in an anisotropic plasma, Planet. Space Sci.,21, 475-483, 1971.

Hudson, P.D., Rotational discontinuities in an anisotropic plasma-II, Planet. Space Sci., 21, 475-483, 1973.

Levy, R.H., H.E. Petschek, and G.L. Siscoe, Aerodynamic aspects of the magnetospheric flow, AIAA J., 2, 2065-2076, 1964.

Mozer, F.S., R.B. Torbert, U.V. Fahleson, C.-G. Fälthammar, A. Gonfalone, A. Pedersen, and C.T. Russell, Direct observation of a tangential electric field component at the magnetopause, Geophys. Res. Lett., 6, 305-308, 1979.

Ogilvie, K.W., T. von Rosenvinge, and A.C. Durney, International sun-earth explorer: A three-spacecraft program, Science, 198, 131-138, 1977.

Paschmann, G., N. Sckopke, G. Haerendel, I. Papamastorakis, S.J. Bame, J.R. Asbridge, J.T. Gosling, E.W. Hones, Jr., and E.R. Tech, ISEE plasma observations near the subsolar magnetopause, Space Sci. Rev., 22, 717-737, 1978.

Paschmann, G., B.U.Ö. Sonnerup, I. Papamastorakis, N. Sckopke, G. Haerendel, S.J. Bame, J.R. Asbridge, J.T. Gosling, C.T. Russell, and R.C. Elphic, Plasma acceleration at the earth's magnetopause: Evidence for reconnection, Nature, 282, 243-246, 1979.

Paschmann, G., N. Sckopke, J.R. Asbridge, S.J. Bame, and J.T. Gosling, Energization of solar wind ions by reflection from the Earth's bow shock, J. Geophys. Res., 85, 4689-4693, 1980.

Petschek, H.E., The mechanism for reconnection of geomagnetic and interplanetary field lines, in: The Solar Wind (R.J. Mackin, Jr., and M. Neugebauer, eds.), pp. 257-263, Pergamon, New York, 1966.

Russell, C.T., The ISEE-1 and -2 fluxgate magnetometers, IEEE Transact. Geosci. Electron., GE-16, 239-242, 1978.

Russell, C.T., and R.C. Elphic, Initial ISEE magnetometer results: magnetopause observations, Space Sci. Rev., 22, 681-715, 1978.

Russell, C.T., and R.C. Elphic, ISEE observations of flux transfer events at the dayside magnetopause, Geophys. Res. Lett., 6, 33-36, 1979.

Scholer, M., F.M. Ipavich, G. Gloeckler, D. Hovestadt, and B. Klecker, Leakage of magnetospheric ions into the magnetosheath along reconnected field lines at the dayside magnetopause, J. Geophys. Res., 86, 1981 (in press).

Sonnerup, B.U.Ö., Acceleration of particles reflected at a shock front, J. Geophys. Res., 74, 1301-1304, 1969.

Sonnerup, B.U.Ö., Magnetopause structure during the magnetic storm of September 24, 1961, J. Geophys. Res., 76, 6717-6735, 1971.

Sonnerup, B.U.Ö., and B.G. Ledley, Electromagnetic structure of the magnetopause and boundary layer, in: Magnetospheric Boundary Layers (B. Battrick, ed.), pp. 401-411, Paris: ESA SP-148, 1979.

Sonnerup, B.U.Ö., Magnetic field reconnection, in: Solar System Plasma Physics, vol. III (L.J. Lanzerotti, C.F. Kennel, and E.N. Parker, eds.), pp. 45-108, Amsterdam: North Holland, 1979.

Su, S.-Y., and B.U.Ö. Sonnerup, First-order orbit theory of the rotational discontinuity, Phys. Fluids, 11, 851-857, 1968.

Vasyliunas, V.M., Theoretical models of magnetic field line merging, 1, Revs. Geophys. Space Phys., 13, 303-336, 1975.

Williams, D.J., and L.A. Frank, ISEE-2 chared particle observations indicative of open magnetospheric field lines near the subsolar region, J. Geophys. Res., 85, 2037-2042, 1980.

Yang, C.K., and B.U.Ö. Sonnerup, Compressible magnetopause reconnection, J. Geophys. Res., 82, 699-703, 1977.

Table 1. Magnetopause Coordinates and Normals

Date		5 Jul 78	3 Aug 78	9 Aug 78	29 Aug 78	3 Sep 78	5 Sep 78	8 Sep 78	12 Sep 78	28 Oct 78	4 Nov 78	11 Sep 78
Time (UT)		14:33	04:21	19:35	12:16	07:19	16:12	00:51	19:44	08:24	13:01	04:10
Orbit		108 OUT	120 OUT	122 IN	131 OUT	133 OUT	134 OUT	135 OUT	137 OUT	156 OUT	159 OUT	289 OUT
Location (GSM)	R	11.7	8.6	14.9	10.0	10.5	10.1	8.7	9.2	12.3	12.8	10.6
	LT	16:00	13:47	16:49	13:00	12:47	12:26	11:41	11:32	09:44	09:05	12:12
	LAT	11.8	17.5	2.4	18.2	20.3	23.0	25.9	26.5	42.7	42.9	21.5
Normal (S/C)	n_x	(m) 0.729	(m) 0.940	(mv) 0.602	(mv) 0.878	(mv) 0.912	(mv) 0.824	(mv) 0.796	(mv) 0.773	(mv) 0.789	(mv) 0.664	(mv) 0.918
	n_y	0.613	0.210	0.783	-0.138	-0.228	-0.257	-0.443	-0.287	-0.541	-0.392	-0.320
	n_z	0.305	0.268	0.157	0.458	0.341	0.505	0.423	0.565	0.291	0.637	0.235

(m) = model normal ; (mv) = minimum variance model ; in the spacecraft coordinate system (very nearly coincident with the GSE system)

Table 2. Characteristics of Magnetopause Crossings

Date		5 Jul 78	3 Aug 78	9 Aug 78	29 Aug 78	3 Sep 78	5 Sep 78[1)]	8 Sep 78	12 Sep 78[1)]	28 Oct 78	4 Nov 78	11 Sep 79[1)]
MS[2)]	B_1 (nT)	49	74	30	43	26	35	54	40	36	18	48
	Δ_{B_1}	-6^o	4^o	6^o	-20^o	-35^o	-12^o	-24^o	-6^o	-64^o	-3^o	-19^o
	ϕ_{B_1}	112^o	107^o	137^o	73^o	83^o	62^o	64^o	64^o	33^o	47^o	66^o
	$n_1(cm^{-3})$	12	66	13	13	11	15	15	16	17	7	21
	$v_1(km\ s^{-1})$	127	141	145	115	143	114	93	81	206	130	103
	β_1	0.3	0.5	0.6	1.1	2.5	1.1	0.6	1.2	1.1	2.0	0.7
	α_1	-0.08	-0.24	-0.05	-0.15	-0.19	-0.18	-0.14	-0.15	-[9)]	-0.25	-0.10
alpha/proton (%)[3)]		(5)	2.5	1.5	4.5	5.0	(5)	2.5	(5)	(5)	(5)	(5)
B_2[4)] (nT)		32	94	24	54	42	32	41	52	47	17	45
$\measuredangle(\underline{B}_1, \underline{B}_2)$[5)]		170^o	110^o	118^o	152^o	160^o	145^o	100^o	104^o	172^o	88^o	130^o
$\lvert\Delta\underline{v}_t^{obs}\rvert_{max}(kms^{-1})$		462	264	168	324	260	128	424	244	225	180	217
6)	Δt_{MP} (s)	60	180	-	30	$\gtrsim$15	-	90	30	30	60	10
	Δt_{BL} (s)	90	150	-	15	30	20	120	120	0	130	55
Magnetosph. ions[7)]		N	Y	Y	N	N	Y	Y	N	N	Y	Y
ϕ[8)]		-	-90^o	-135^o	-	-	-135^o	-110^o	-	-	-135^o	-90^o

Footnotes for Table 2.

(1) ISEE-2 data. All other cases are ISEE-1 data.

(2) Data for magnetosheath reference point (B_1 , Λ_{B1} , Φ_{B1}: magnitude, elevation and azimuth angle (in S/C coordinates) of magnetic field; n_1 , v_1: density and bulk speed ; β_1: ratio of plasma and magnetic field pressures; α_1: pressure anisotropy factor).

(3) Alpha particle abundance in the solar wind. Numbers in parenthesis are assumed values, the others are measured.

(4) Magnetic field strength on magnetopsheric side of magnetopause.

(5) Angle between the vectors $\underline{B}_1$ and $\underline{B}_2$.

(6) Duration of magnetopause and boundary layer encounters, if well defined.

(7) Y indicates presence of energetic ($\gtrsim$ 5 keV) ions appearing as separate component.

N indicates either absence of ions or absence of clear separation.

(8) Streaming direction of energetic ions. Φ is the azimuth angle in the spacecraft system.

(9) α_1 not determined because of large Λ_{B1} .

FIGURE CAPTIONS

Figure 1(a) Meridional view of the reconnection configuration for anti-parallel external and internal magnetic fields. The magnetic field lines are shown as solid lines. The magnetopause (MP) is shown as a current layer of finite thickness, with an adjoining boundary layer (BL) of comparable thickness. Magnetosheath and magnetosphere are located to the left and right of the magnetopause, respectively. Those magnetosheath and magnetospheric field lines connected to the separator (or X-line) form the outer (S1) and inner (S2) separatrix, respectively. The magnetic field normal component B_n is negative north of the separator and positive south of it. Dashed lines are stream lines and the heavy arrows indicate the plasma flow speed outside and inside the magnetopause. The reconnection electric field, E_t, is aligned with the magnetopause current I. All except one of the ISEE crossings discussed in this paper were located north of the separator.

(b) Front view of the reconnection configuration for a case with substantial positive y-component of the magnetosheath magnetic field. Under these circumstances the separator (X-line), shown as the dot-dash line, is tilted upward on the postnoon side. Magnetosheath portions of magnetic field lines are shown as solid lines, magnetosphere portions as dashed lines. Tangential components of magnetic field and plasma velocity are denoted by $\underline{B}_t$ and $\underline{v}_t$, respectively. Index 1 refers to the magnetosheath side, index 2 to the magneto-

sphere side. The location of the only ISEE magnetopause crossing south of the separator discussed in this paper (August 9, 1978) is shown by the symbol B. For comparison, the 8 September, 1978, crossing is marked by the symbol A.

Figure 2 Plasma and magnetic field data from ISEE-1 (top) and ISEE-2 (bottom) for a 36-min interval on 8 September 1978, during which the satellites moved from the outer magnetosphere ("ring current" = RC) through the boundary layer (BL) and magnetopause (MP) into the magnetosheath (MS). The crossings of the outer separatrix are denoted by S. The plasma data are from the 3D analyzer and are spaced 12s apart. The upper curve in the top panels, N_p , is the total plasma number density (cm^{-3}); the lower curve, $\tilde{N}_p$, is the density (cm^{-3}) of the energetic (13 - 40 keV) ions; V_p and V_z are the magnitude and GSM z-component of the bulk velocity ($km\ s^{-1}$). The solid curve in the bottom panel of the ISEE-1 data is the total plasma pressure P (in units of 10^{-9} N m^{-2}). The magnetic field data are shown with 9s resolution: B_z (nT) is the GSM z-component and B (dotted curve in bottom panel) the field strength (nT, right-hand scale) or the field pressure (in units of 10^{-9} N m^{-2}, left-hand scale). Universal times UT (in hours), and geocentric radial distances R (in earth radii) are given at the bottom. The spacecraft local time and GSM latitude were ~ 1140 hours and ~ $+26^{o}$, respectively. The figure shows that large plasma flow speeds are observed during each magnetopause/boundary layer encounter

Figure 3 Inferred radial motion of the magnetopause, boundary layer, and outer separatrix, relative to the ISEE satellite pair, on 8 September, 1978. Several times have been marked to facilitate comparison with Figure 2.

Figure 4 ISEE-1 plasma and magnetic field data for one hour on 9 August 1978. The plasma density, N_p, bulk speed, V_p, and pressure P are from the 2D instruments and are shown every 12s. Only the V_z component of the flow is from the 3D instrument and is shown every 48s. The magnetic field is represented in terms of its magnitude B and the two tangential components, B_L and B_M, in the LMN boundary normal coordinate system (defined in the text). Universal times and spacecraft coordinates are indicated at the bottom. The period of interest is that between 19:34 UT and 19:53 UT during which the satellite stayed within the magnetopause almost continuously. The entire interval is characterized by large flow speeds with a negative (i.e. southward directed) V_z component. At 19:53 UT the spacecraft reentered the magnetosheath, before finally crossing into the magnetosphere near 20:10 UT.

Figure 5 ISEE-1 plasma and magnetic field data for magnetopause crossings on 3 September 1978. The format is the same as that of Figure 3, except that the magnetic field direction is indicated only in terms of B_z as in Figure 2. High flow speeds, directed northward, are detected at each of the magnetopause and boundary layer crossings.

Figure 6 ISEE-1 plasma and magnetic field data for magnetopause crossings on 28 October 1978 in the same format as Figure 4. The principal magnetopause encounter (08:21 UT to 08:23 UT) is a succession of complete outward/inward/outward crossings, as illustrated by the behaviour of B_z. Enhanced flow speeds are again detected.

Figure 7 Results of the tangential component tests (Ia, b, c) for the ISEE-1 and ISEE-2 magnetopause/boundary layer crossings on 8 September 1978. Each vector represents the ratio of the measured change in tangential plasma velocity $\Delta \underline{v}_t^{obs}$ to the change $|\Delta \underline{v}_t^{th}|$ predicted form the measured change in tangential magnetic field, according to Eq. 7. The plasma velocity and magnetic field changes, relative to a fixed point in the magnetosheath, were computed for each measurement within the magnetopause and boundary layer, which passed the criteria stated in the Appendix. Since the ISEE-1 and -2 crossings were quite different and ISEE-2 had a data gap right at the magnetopause (cf. Figure 2), the vectors for ISEE-1 and -2 do not necessarily refer to the same relative locations. Tangential components were obtained using a local magnetopause normal derived from minimum variance analysis. The angles between the vectors and the horizontal (dashed line) indicate deviations from the predicted directions $(\Delta \underline{v}_t^{th})$. The vectors point consistently to the right, indicating $B_n < 0$. Unit length of the vectors indicates perfect agreement with the predicted magnitude $|\Delta v_t^{th}|$. Absolute magnitudes range from ~ 200

to ~425 km s^{-1}. Since the theoretical direction $\Delta \underline{v}_t^{th}$ changes continuously throughout the magnetopause crossing, the orientation of the vectors in this figure do not coincide with their actual orientation in space.

Figure 8 Result of the tangential component test for the ISEE-1 crossing on 9 August 1978. For an explanation see Figure 7 and text. The vectors point to the left, indicating $B_n > 0$, absolute magnitudes of vectors range from ~ 100 to 290 km s^{-1}.

Figure 9 Results of the tangential component test for the remaining 9 cases. The scarcity of vectors in several of the cases is due to brief magnetopause durations (compared with the 48s resolution of the plasma velocity obtained in all low bit rate crossings) or the rejection of substantial numbers of measurements (see Appendix).

Figure 10 Summary of tangential component tests for the 11 cases studied. Each vector now represents one entire crossing and is obtained by averaging the individual vectors shown for the 11 cases in Figures 7, 8, and 9.

Figure 11 Time sequence of ion energy spectra spaced 12s apart, for the time interval 00:40 UT to 01:00 UT on 8 September 1978. Count rates are in s^{-1}, energies in keV. Spectra were summed over the range (~ 180^{o}) of azimuth where the energetic ions are observed (cf. Figure 12). The various regions encountered during this interval are indicated (cf. Figure 2). Two features are emphasized: (i) a high-energy

($E \gtrsim 5$ keV) component persists well into the magnetosheath and terminates at 00:56 UT, at the outer separatrix S; these ions are interpreted as magnetospheric; (ii) a secondary peak near 1 keV (marked "R") is also observed in the magnetosheath until 00:56 UT; these ions have probably been reflected off the magnetopause .

Figure 12 Relief plot of two-dimensional count rate distributions in the GSE (v_x , v_y) plane for velocities up to 2500 km s^{-1}, measured just after the final magnetopause crossing on 8 September 1978. The plot is based on a one-minute accumulation of count rates in 16 velocity and 8 azimuth channels. The three peaks near the center represent the main magnetosheath plasma (1), ions (2) which have been reflected at the magnetopause, and a small contribution of He^+ ions (3), respectively. The crescent-shaped distribution at high energies (4) is interpreted as ions of magnetospheric (ring current) origin leaking out along reconnected field lines. They are seen to move preferentially antiparallel to the projected magnetic field $\underline{B}$, as expected for a crossing north of the X-line (Figure 1b). The abrupt outer termination of the distribution of energetic ions reflects the high-energy cutoff of the instrument at 40 keV.

Figure 13 Relief plot of two-dimensional count rate distribution measured just outside the magnetopause on 9 August 1978. In this case the high-energy component, interpreted as ions of magnetospheric origin, is observed to move parallel to the magnetic field, as expected for a crossing south of the

X-line (Figure 1b). Maximum particle velocities are 2500 km s^{-1}.

Figure 14 View from the earth of the vectors $\underline{E}_t/|B_n|$ relative to the total magnetopause current $\underline{I}$ for the 11 magnetopause crossings analyzed. For each crossing, the two vectors $\underline{E}_t/|B_n|$ and $\underline{I}$ have been rotated, maintaining the angle between them, until I is horizontal. $\underline{E}_t$ is the tangential electric field (in mV/m), $\underline{B}_n$ the magnitude of the normal field component (in nT), at the magnetopause.

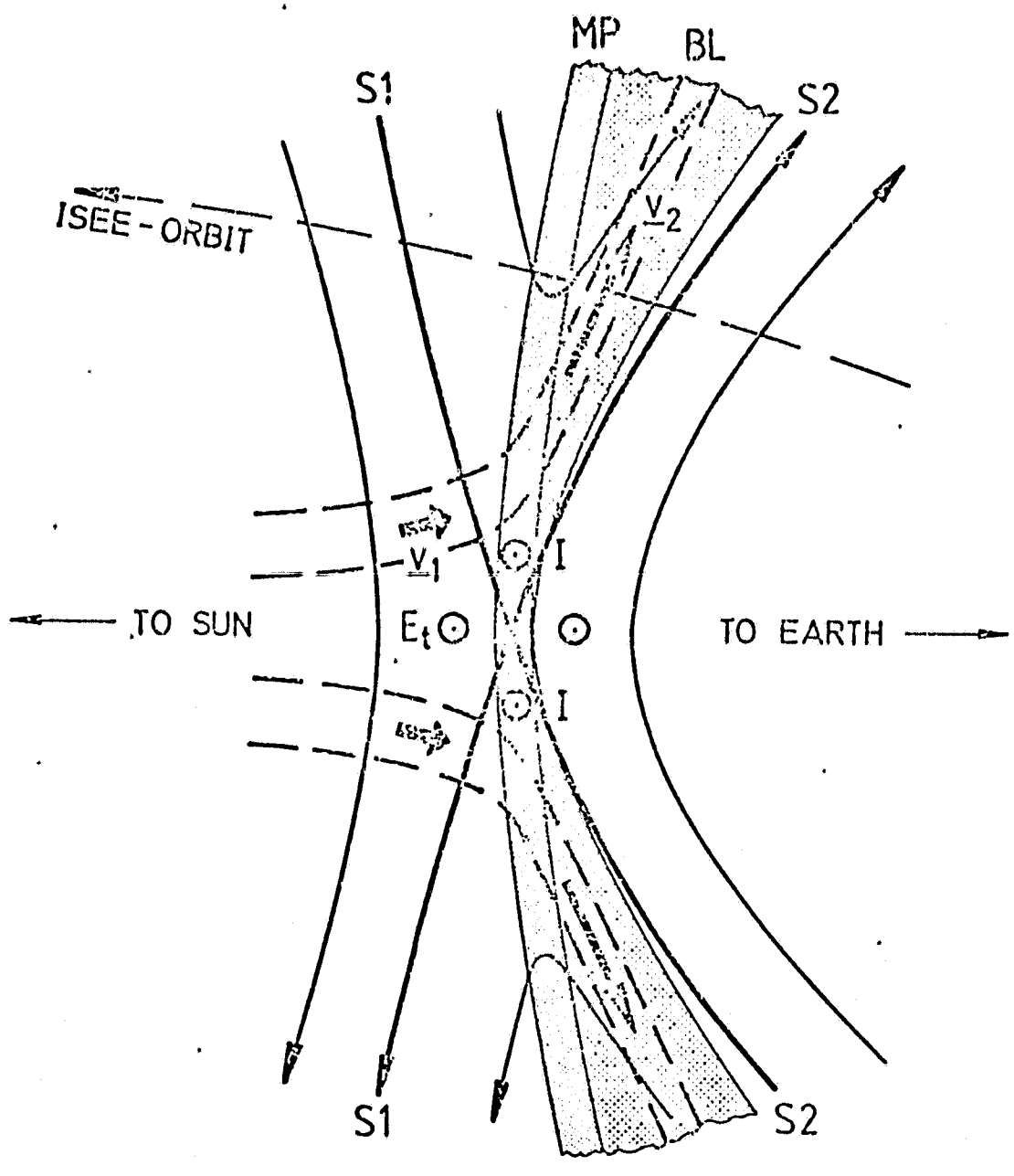
MP
BL
S1
S2
ISEE - ORBIT
$\underline{V}_2$
$\underline{V}_1$
I
I
TO SUN
E_t
TO EARTH
S1
S2

Figure 1a

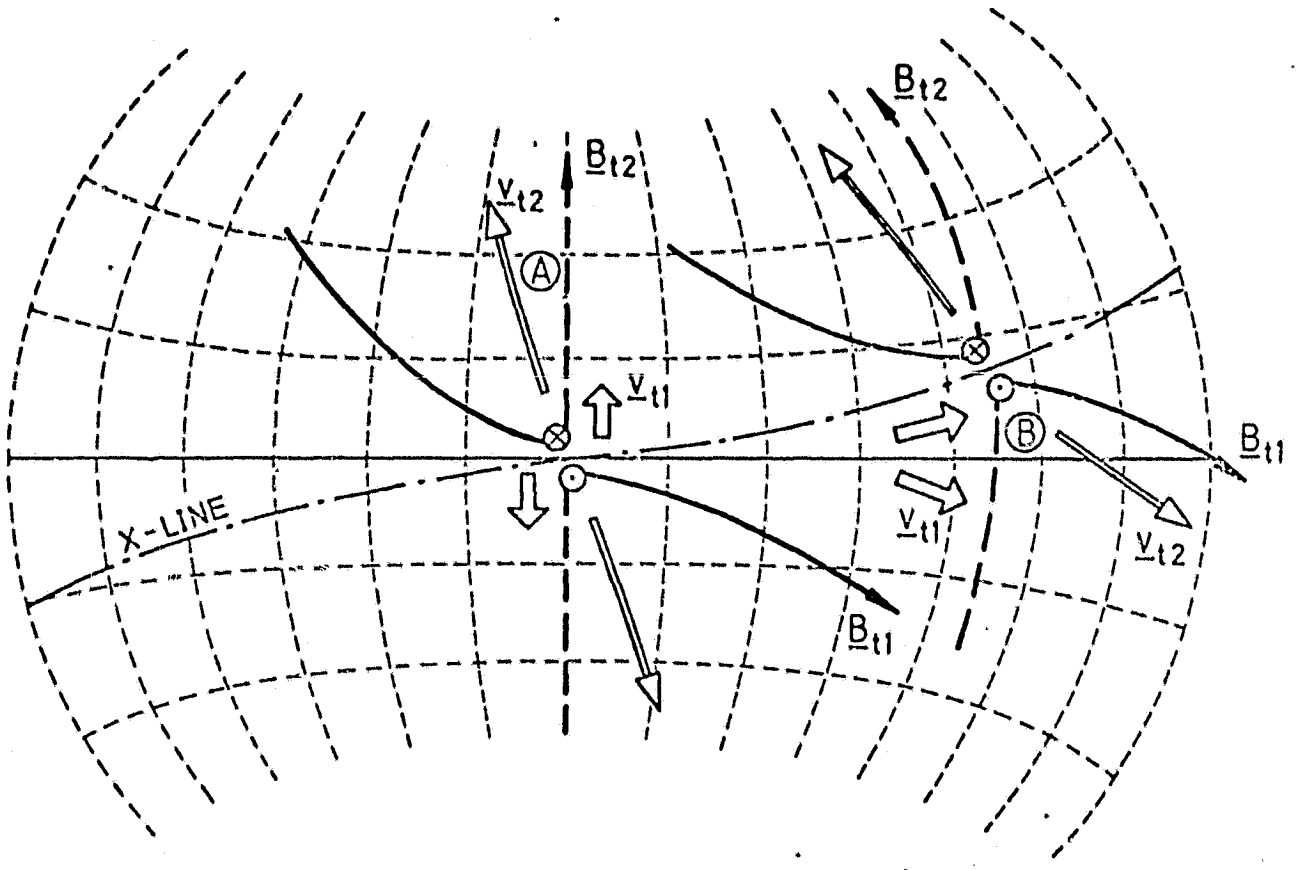

Figure 1b

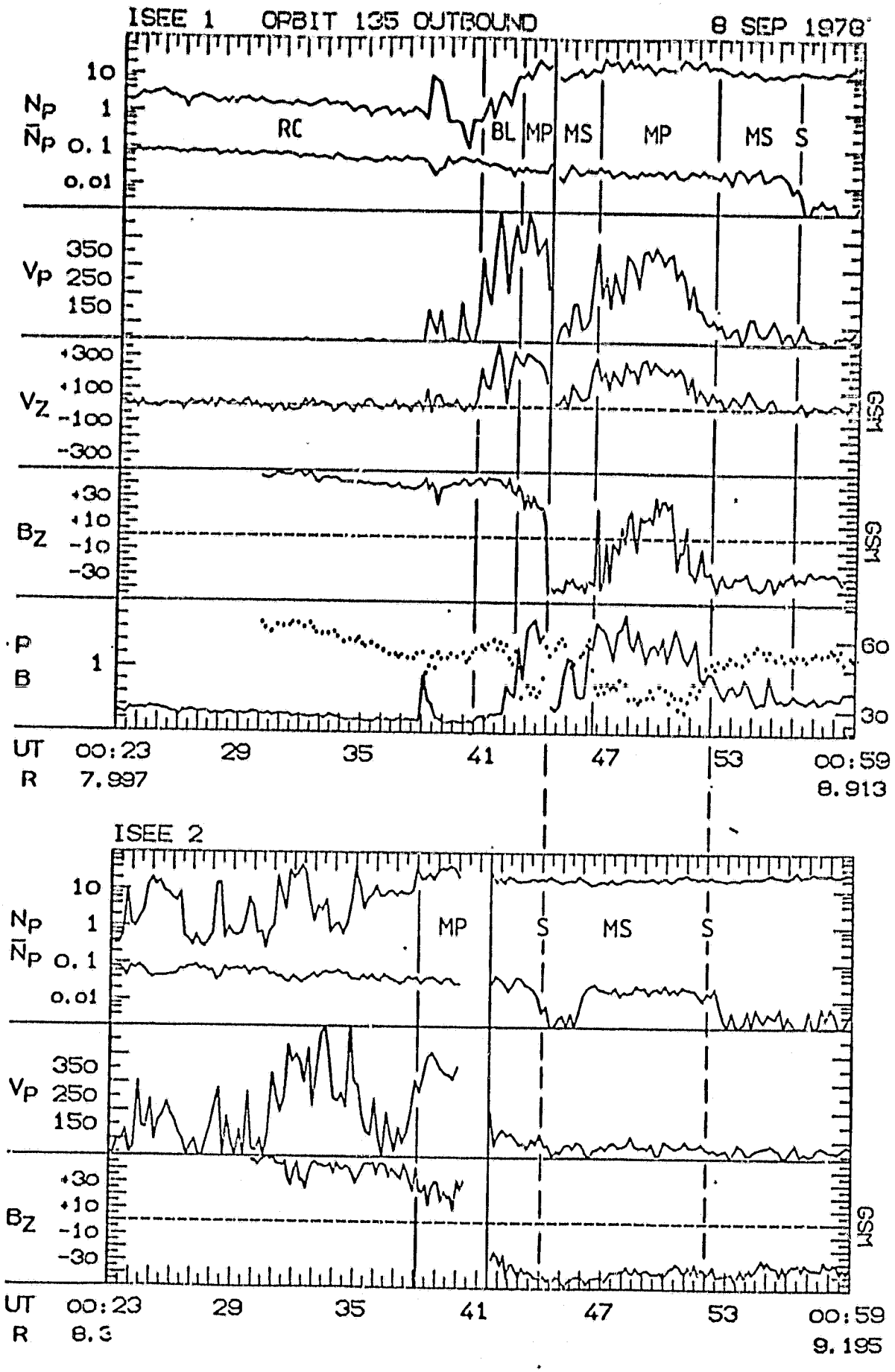
ISEE 1 ORBIT 135 OUTBOUND 8 SEP 1978
10
N_P 1
$\bar{N}_P$ 0.1
0.01
RC
BL
MP
MS
MP
MS
S
350
V_P 250
150
+300
+100
V_Z -100
-300
GSM
+30
+10
B_Z -10
-30
GSM
P
B
1
60
30
UT 00:23 29 35 41 47 53 00:59
R 7.997
8.913
ISEE 2
10
N_P 1
$\bar{N}_P$ 0.1
0.01
MP
S
MS
S
350
V_P 250
150
+30
+10
B_Z -10
-30
GSM
UT 00:23 29 35 41 47 53 00:59
R 8.3
9.195

Figure 2

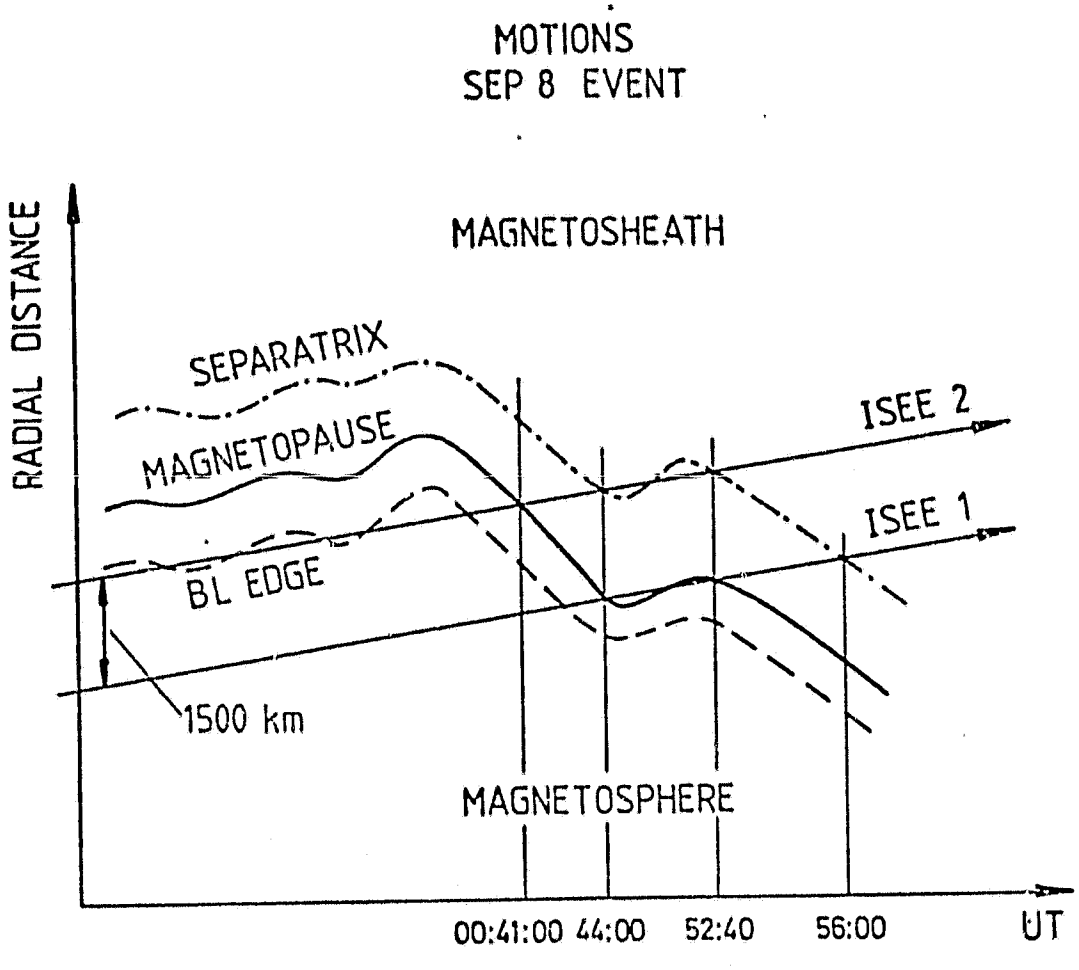
MOTIONS
SEP 8 EVENT
MAGNETOSHEATH
RADIAL DISTANCE
SEPARATRIX
MAGNETOPAUSE
ISEE 2
ISEE 1
BL EDGE
1500 km
MAGNETOSPHERE
00:41:00
44:00
52:40
56:00
UT

Figure 3

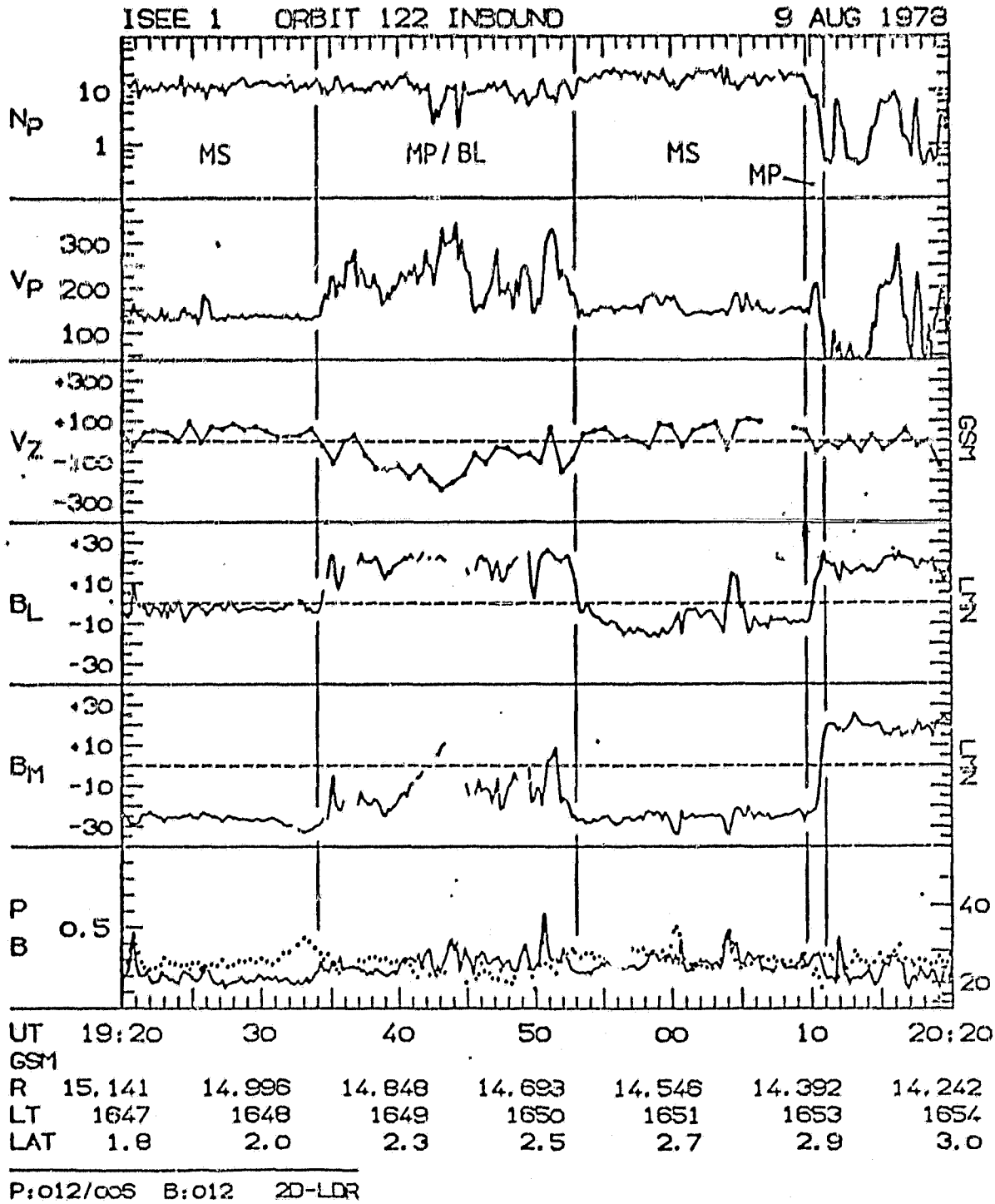
ISEE 1 ORBIT 122 INBOUND 9 AUG 1978
N_P
10
1
MS
MP/BL
MS
MP
V_P
300
200
100
V_Z
+300
+100
-100
-300
GSM
B_L
+30
+10
-10
-30
LMN
B_M
+30
+10
-10
-30
LMN
P
B
0.5
40
20
UT 19:20 30 40 50 00 10 20:20
GSM
R 15.141 14.996 14.848 14.693 14.546 14.392 14.242
LT 1647 1648 1649 1650 1651 1653 1654
LAT 1.8 2.0 2.3 2.5 2.7 2.9 3.0
P:012/005 B:012 2D-LDR

Figure 4

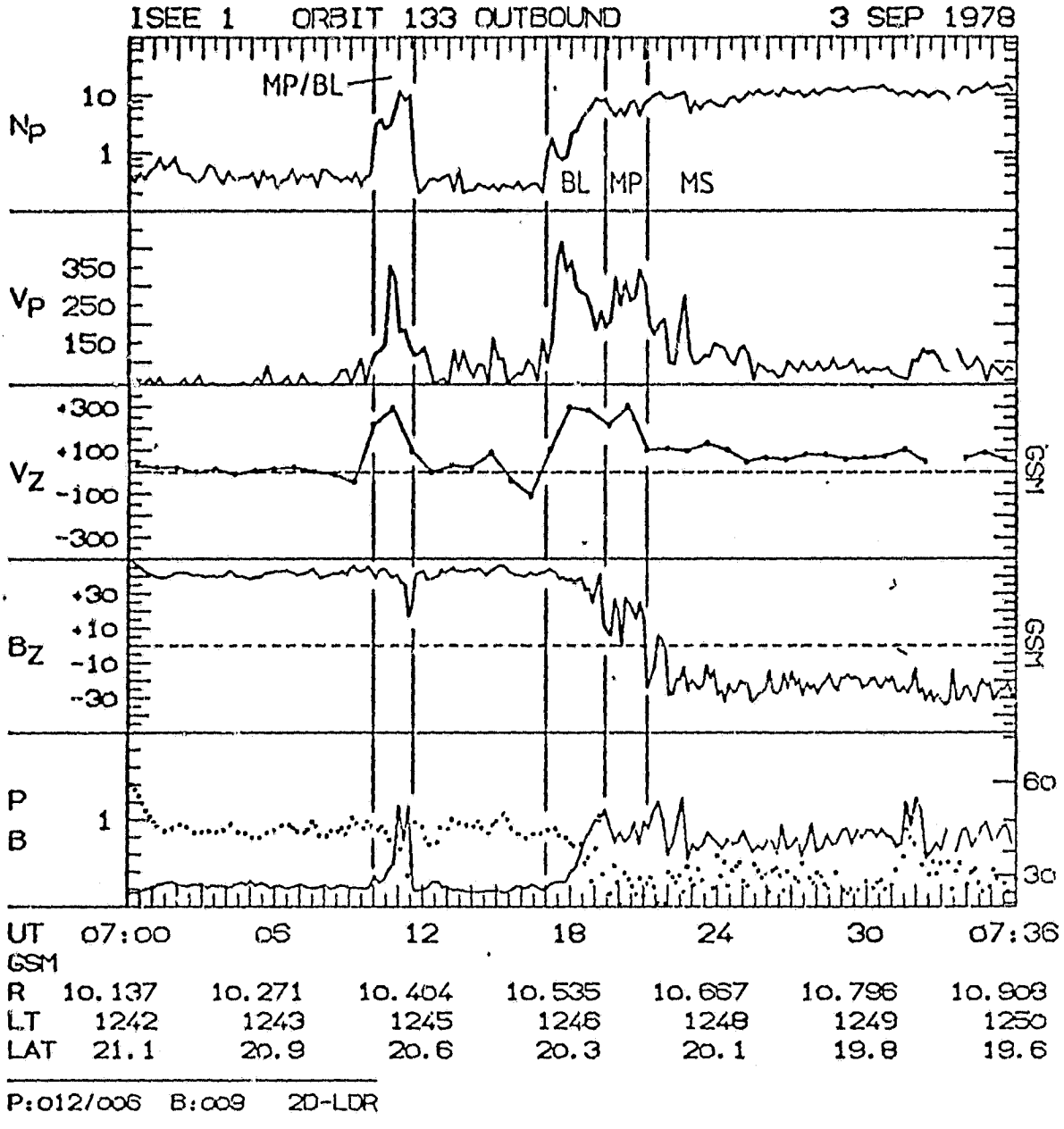
ISEE 1 ORBIT 133 OUTBOUND 3 SEP 1978
MP/BL
BL
MP
MS
Np
10
1
VP
350
250
150
VZ
+300
+100
-100
-300
GSM
BZ
+30
+10
-10
-30
GSM
P
B
1
60
30
UT 07:00 06 12 18 24 30 07:36
GSM
R 10.137 10.271 10.404 10.535 10.667 10.796 10.908
LT 1242 1243 1245 1246 1248 1249 1250
LAT 21.1 20.9 20.6 20.3 20.1 19.8 19.6
P:012/006 B:009 20-LDR

Figure 5

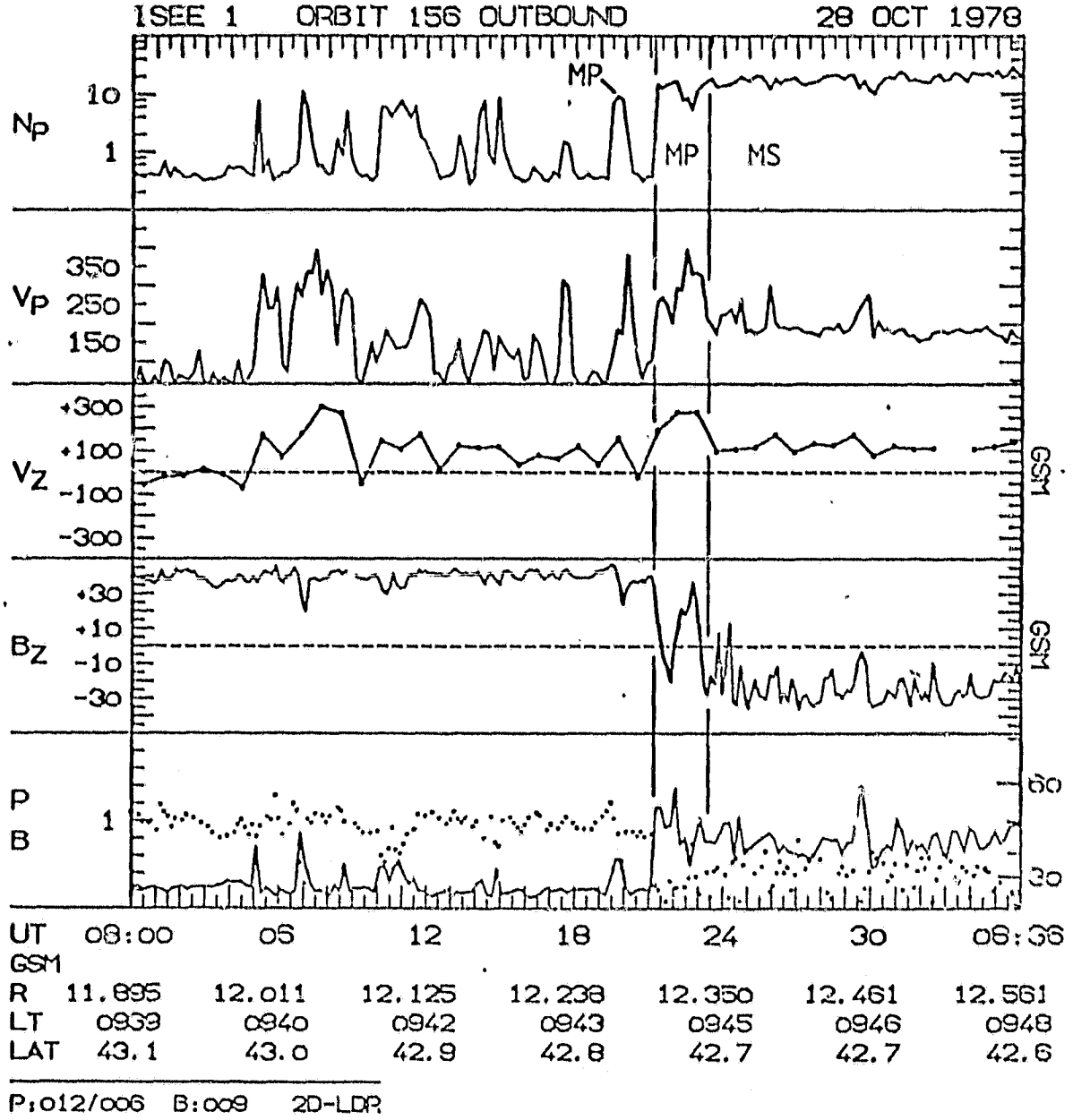
ISEE 1 ORBIT 156 OUTBOUND 28 OCT 1978
MP
MP
MS
Np
10
1
Vp
350
250
150
Vz
+300
+100
-100
-300
GSM
Bz
+30
+10
-10
-30
GSM
P
B
1
60
30
UT 08:00 05 12 18 24 30 08:36
GSM
R 11.895 12.011 12.125 12.238 12.350 12.461 12.561
LT 0939 0940 0942 0943 0945 0946 0948
LAT 43.1 43.0 42.9 42.8 42.7 42.7 42.6
P:012/006 B:009 2D-LDR

Figure 6

8 SEP 78
ISEE - 1

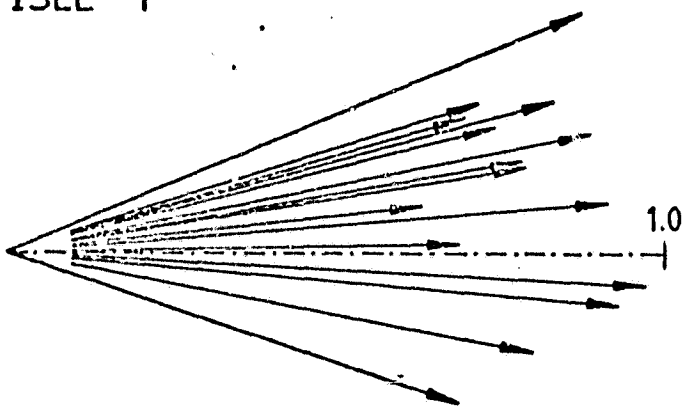

ISEE - 2

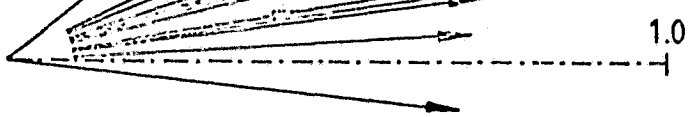

Figure 7

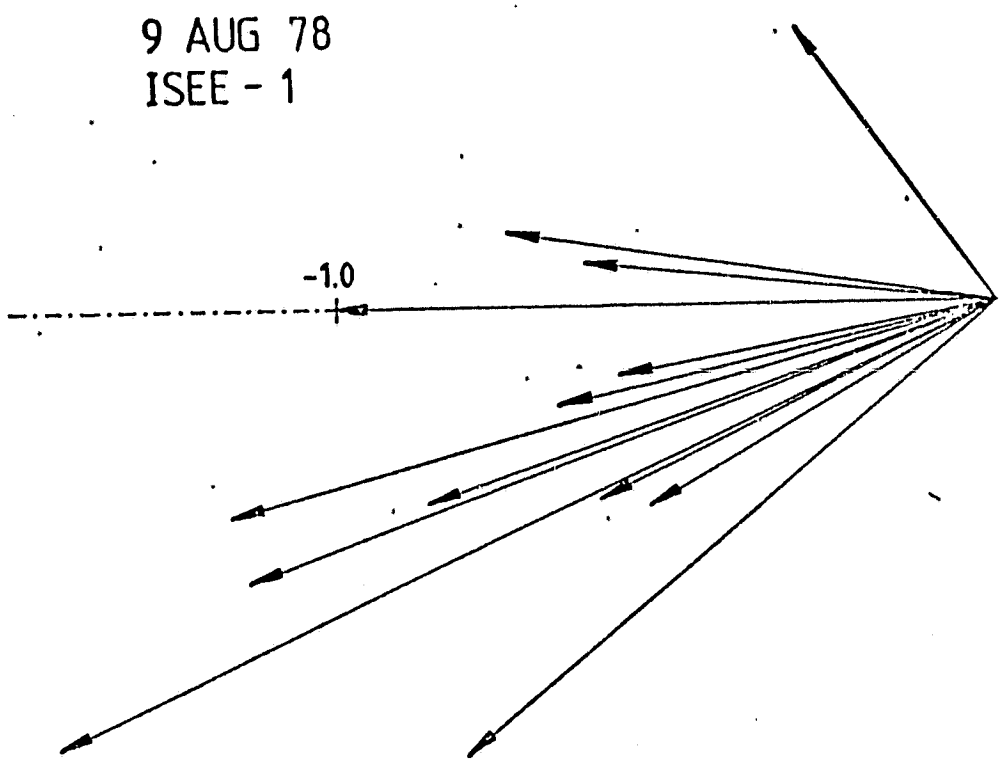

Figure 8

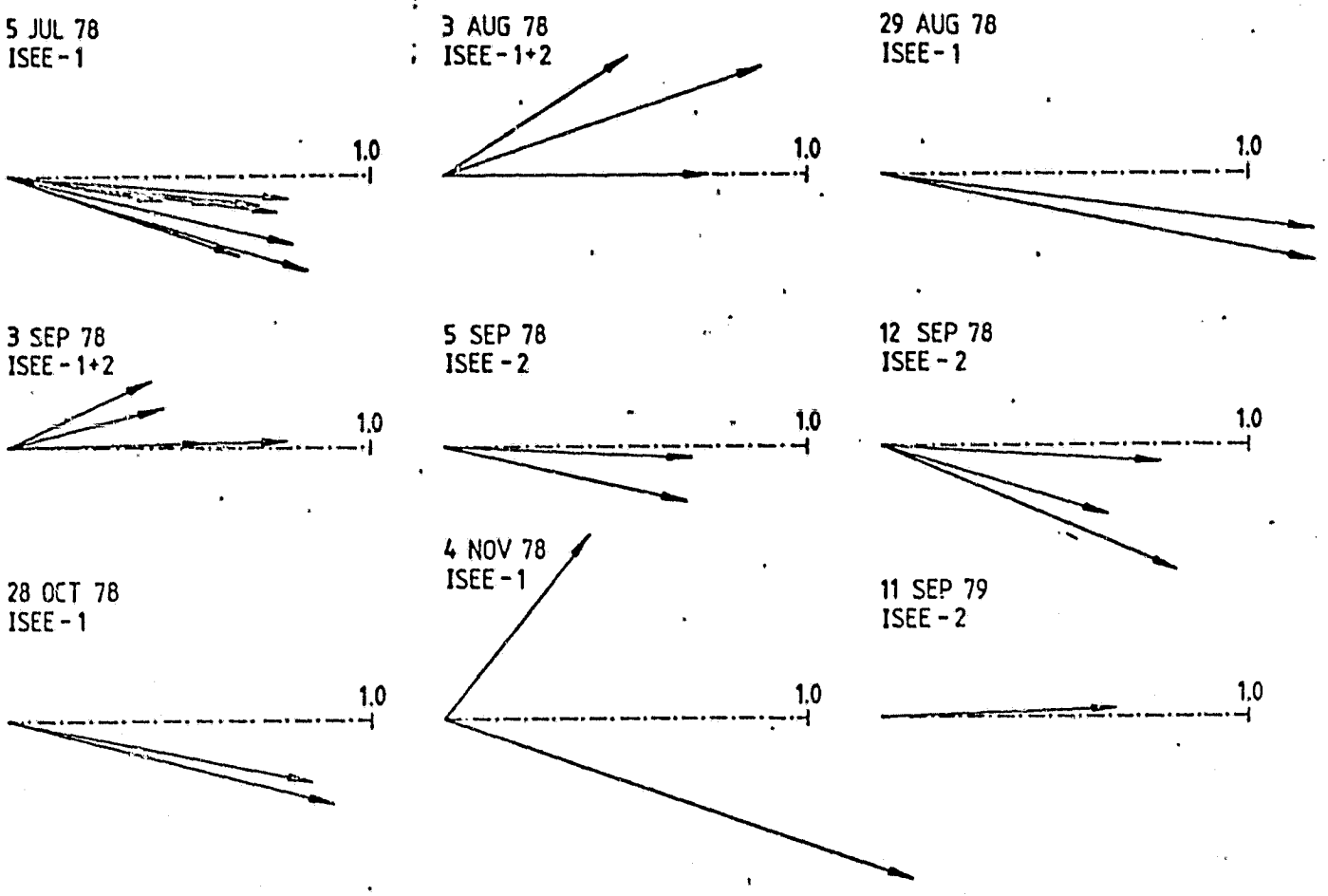
5 JUL 78
ISEE - 1
1.0
3 AUG 78
ISEE - 1+2
1.0
29 AUG 78
ISEE - 1
1.0
3 SEP 78
ISEE - 1+2
1.0
5 SEP 78
ISEE - 2
1.0
12 SEP 78
ISEE - 2
1.0
28 OCT 78
ISEE - 1
1.0
4 NOV 78
ISEE - 1
1.0
11 SEP 79
ISEE - 2
1.0

Figure 9

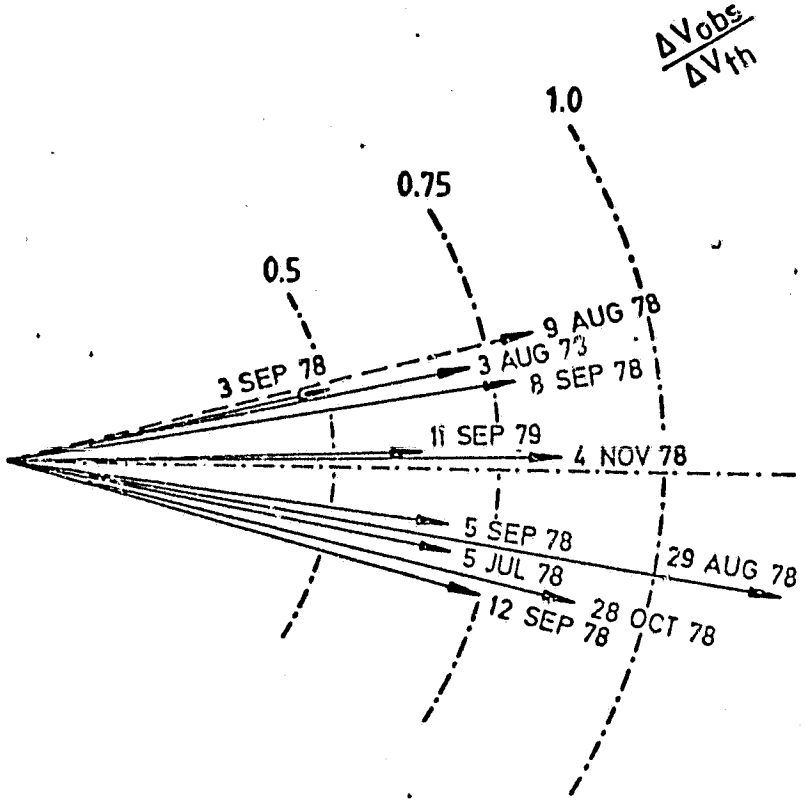
ΔVobs/ΔVth
1.0
0.75
0.5
9 AUG 78
3 AUG 73
8 SEP 78
3 SEP 78
11 SEP 79
4 NOV 78
5 SEP 78
29 AUG 78
5 JUL 78
28 OCT 78
12 SEP 78

Figure 10

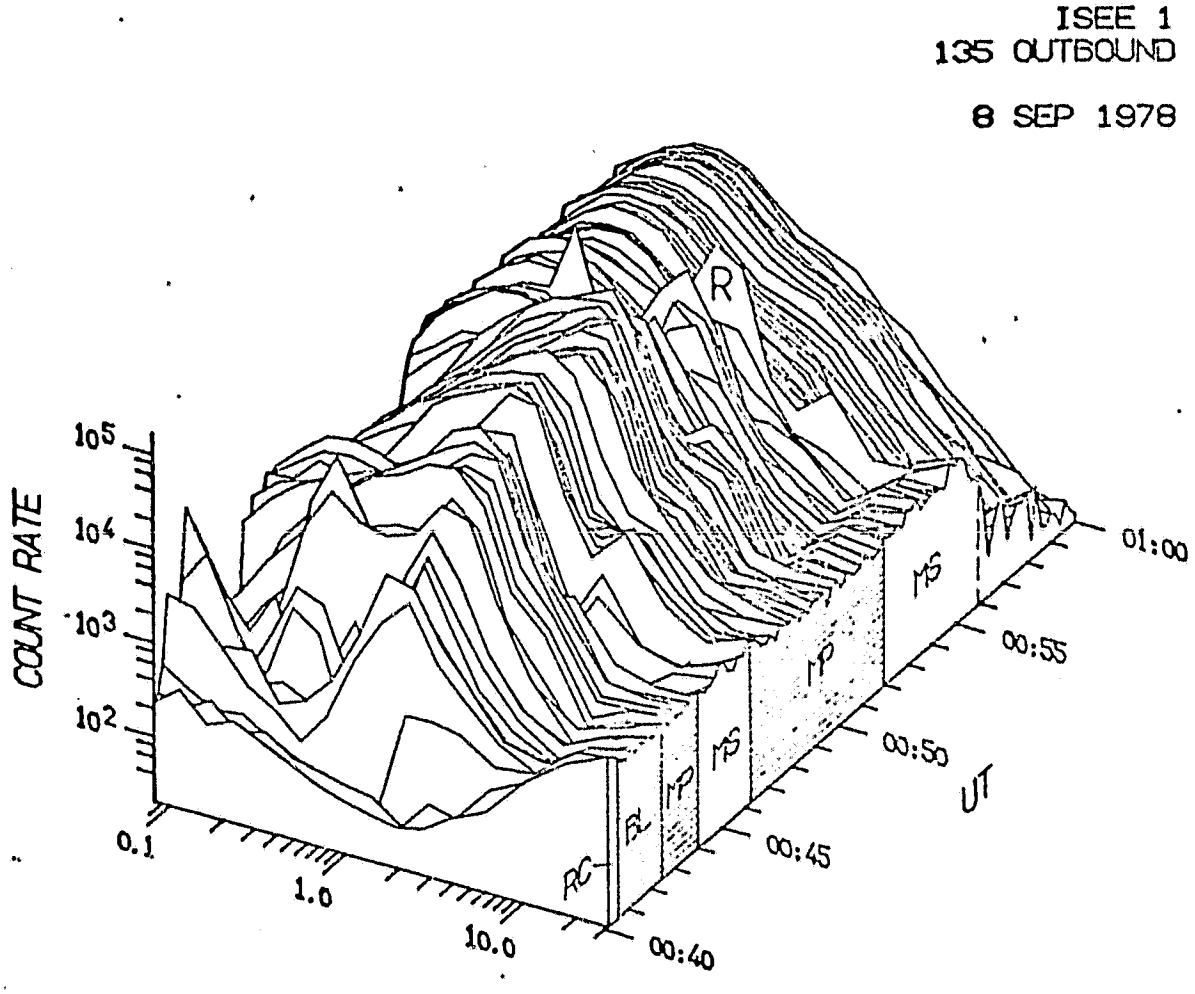
ISEE 1
135 OUTBOUND
6 SEP 1978
COUNT RATE
10^5
10^4
10^3
10^2
0.1
1.0
10.0
R
RC
FL
MP
MS
MP
MS
00:40
00:45
00:50
00:55
01:00
UT

Figure 11

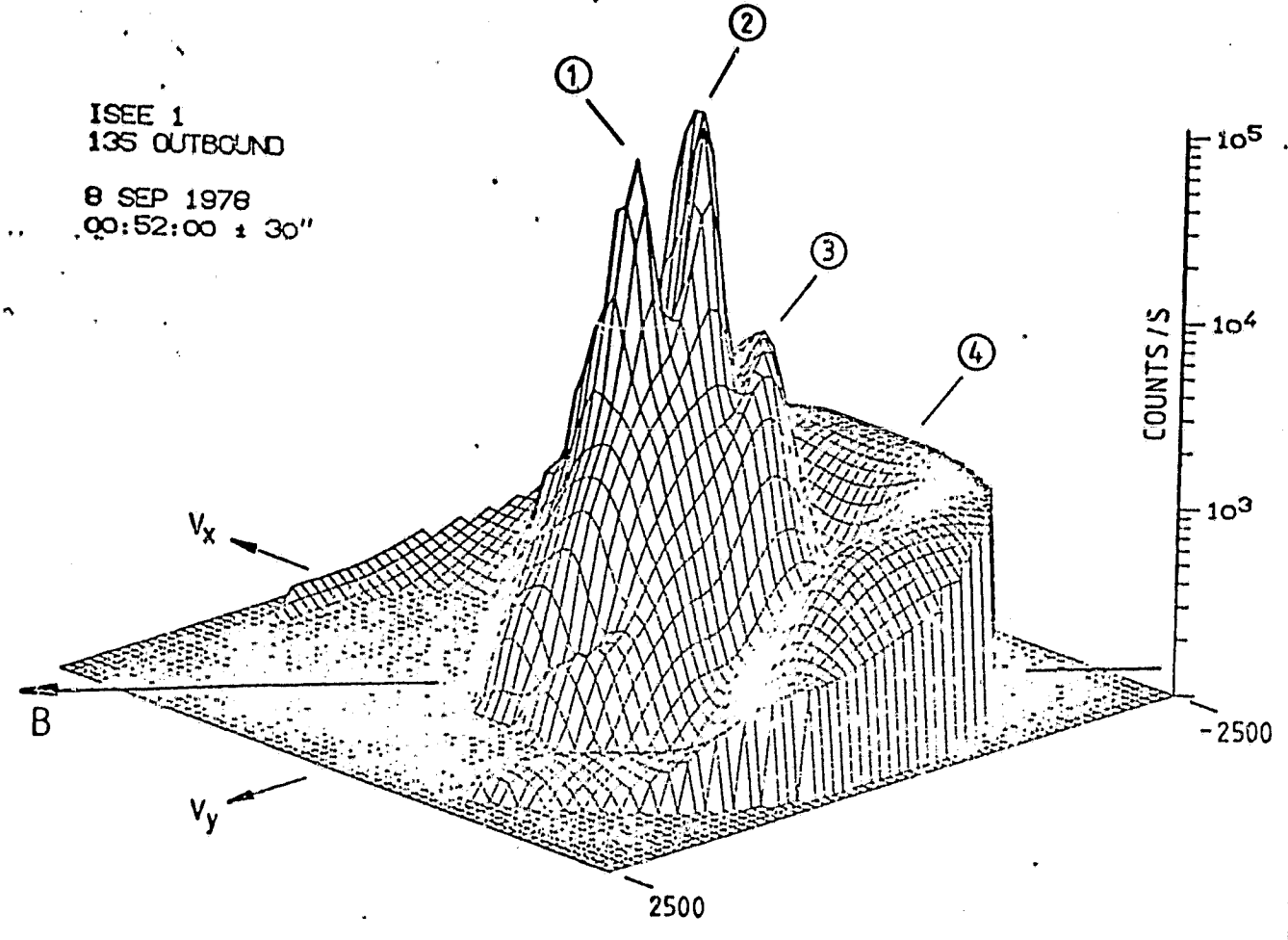

Figure 12

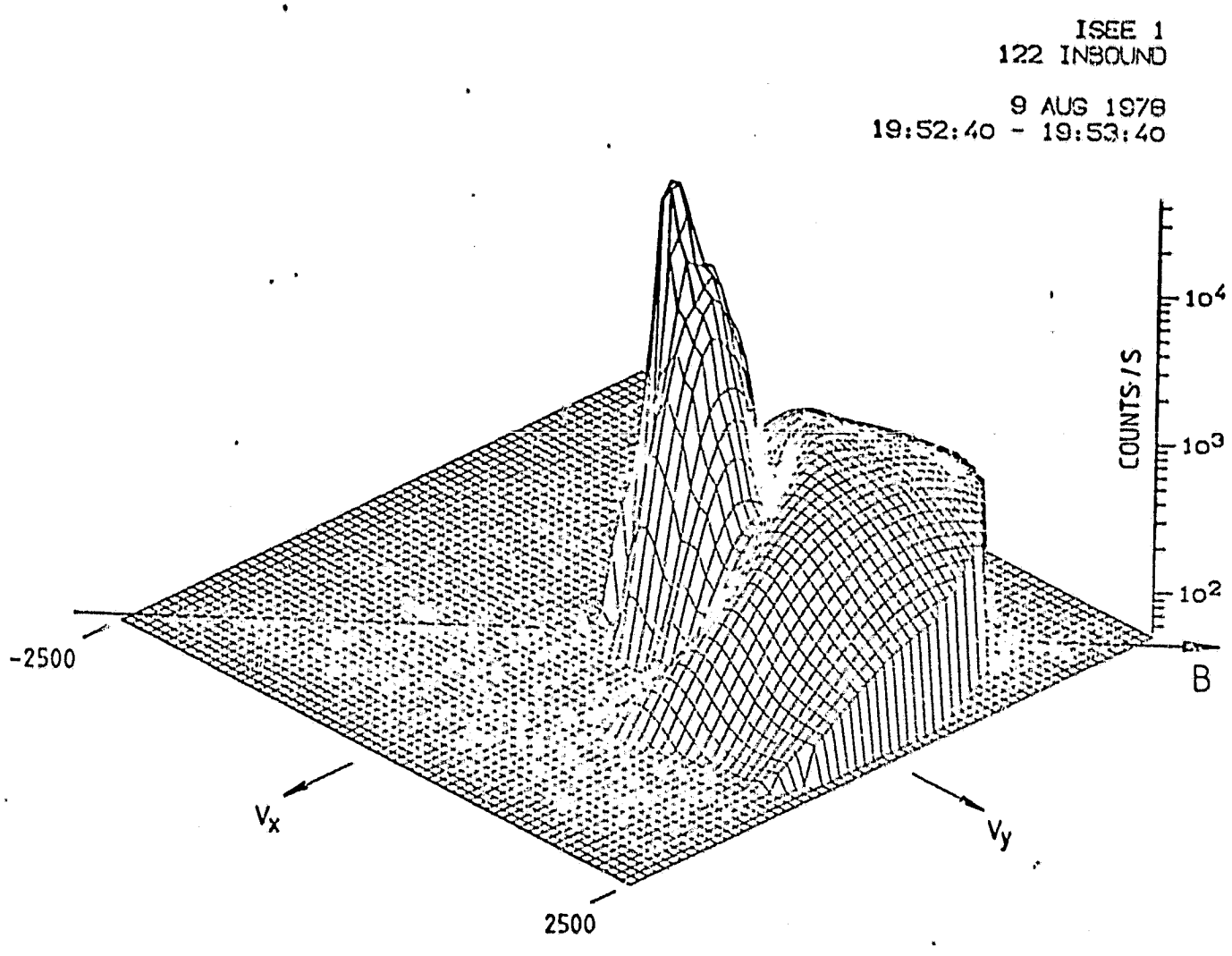

Figure 13

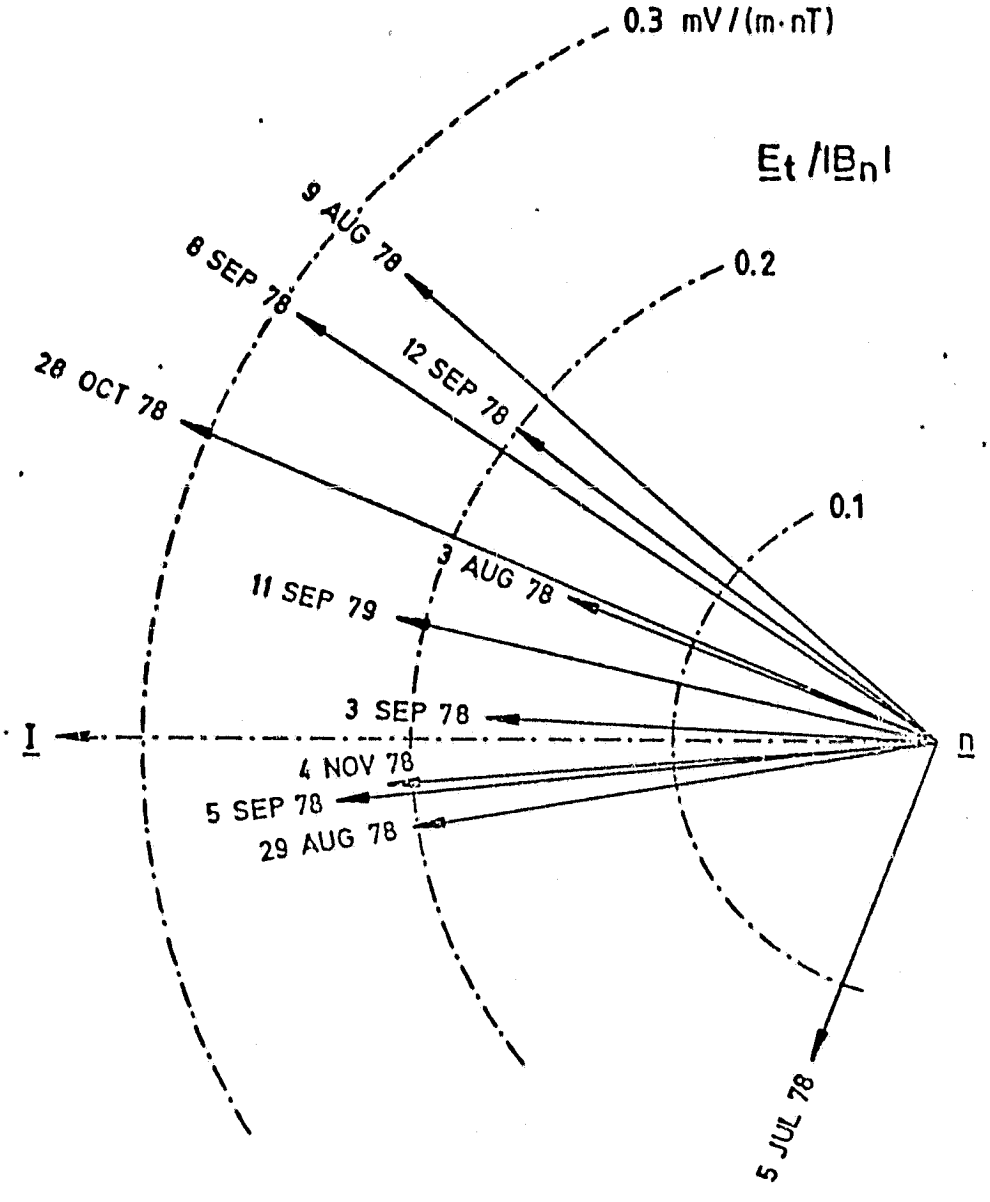
0.3 mV/(m·nT)
$E_t/|B_n|$
0.2
0.1
9 AUG 78
8 SEP 78
12 SEP 78
28 OCT 78
3 AUG 78
11 SEP 79
3 SEP 78
I
n
4 NOV 78
5 SEP 78
29 AUG 78
5 JUL 78

Figure 14